Cardiac hypertrophy may be an adaptive response of the heart to haemodynamic overload, as in hypertension. To evaluate the contribution of increased blood pressure to cardiac hypertrophy and fibrosis, GCA KO mice were treated with hydralazine. Unexpectedly, we found that, despite its antihypertensive actions, hydralazine potentiated cardiac hypertrophy in GCA KO mice. We further investigated the underlying mechanism of this effect by genetically deleting AT_1 or AT_2 receptors.

Methods

Animals and treatments

The animal care and all experimental protocols were reviewed and approved by the Animal Research Committee in Kyoto University Graduate School of Medicine.

Experiment 1. Male homozygous GCA KO and WT mice used in this experiment ($n = 7$–14 each group) were generated by methods described previously (Lopez *et al.*, 1995). The genetic background of the mice was C57BL/6. Treatments were started when mice were 12 weeks of age. Hydralazine (Sigma, Osaka, Japan) was administered in drinking water (≈24 mg·kg^{-1}·day^{-1}) over a 5 week period; the solution was replaced on alternate days. Control mice received drinking water alone. Systolic blood pressure (SBP) was measured prior to commencement and at weekly intervals during the 5 week experiment after which animals were killed.

Experiment 2. The genetic background of the mice lacking the AT_{1a} gene (AT_1 KO) mice was C57BL/6. Male homozygous AT_1 KO mice and mice with both GCA and AT_1 KO ('double' KO; GCA/AT_1 DKO) used in this experiment ($n = 6$–7 each group) were generated by methods described previously (Li *et al.*, 2002; 2004). The other experimental procedures were the same as those described in *Experiment 1.*

Experiment 3. The genetic background of the AT_2-deficient (AT_2 KO) mice was FVB/N. Male homozygous AT_2 KO and GCA and AT_2 double KO (GCA/AT_2 DKO) mice used in this experiment ($n = 7$–8 each group) were generated by methods described previously (Li *et al.*, 2009). The other experimental procedures were the same as those described in *Experiment 1.*

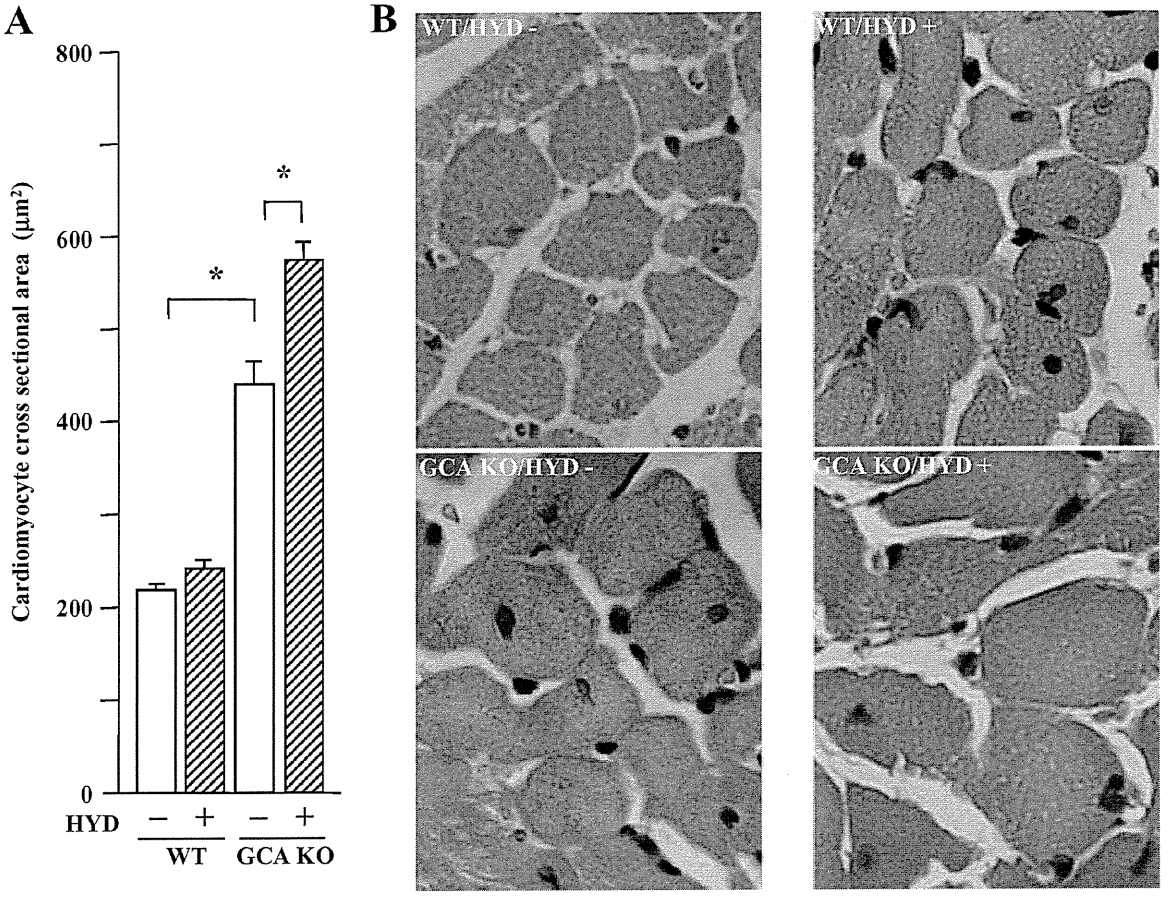

Figure 2 Cardiomyocyte cross-sectional areas in wild-type (WT) and guanylyl cyclase-A (GCA) knockout (KO) mice. Hydralazine (HYD) was administered in drinking water (≈24 mg·kg^{-1}·day^{-1}) for 5 weeks, while the mice in control groups received drinking water only. Morphometry of left ventricular myocytes was performed to measure the myocyte cross-sectional area. Values are means ± SEM ($n = 7$–14). *$P < 0.05$. (A) Results of cardiomyocyte cross-sectional areas with or without HYD treatment. (B) Representative histological findings of cardiomyocytes in different experimental groups. Original magnification: ×400. HYD −: control, without HYD; HYD +, with HYD.

Heart rate and SBP measurement
Heart rate (HR) and SBP were measured in conscious mice using a computerized tail-cuff method (Softron, Co., Ltd., Tokyo, Japan) at 10:00–14:00. The validity of this system has been established in our laboratory (Li *et al.*, 2002; 2004; 2009; Nakanishi *et al.*, 2005).

Determination of heart and left ventricular weights
Hearts were dissected and the weights of the total heart (HW) and left ventricle (LVW) were measured. The ratios of HW or LVW to the body weight (HW/BW and LVW/BW) were calculated and used as an index of cardiac hypertrophy.

Measurement of cardiomyocyte cross-sectional areas
A section from each left ventricle was fixed in 10% neutral formalin over several days and dehydrated with graded concentrations of alcohol for embedding in paraffin. Paraffin slices from each heart were stained with haematoxylin-eosin. Morphometry of left ventricular myocytes was performed according to the method described in previous reports (Sanada *et al.*, 2003). The cross-sectional area was measured using an image analysing system (KS 400 Imaging System; Carl Zeiss Vision, Eching, Germany) in cardiomyocytes that were cut transversely and had a visible nucleus and an unbroken cellular membrane. The outer borders of the cardiomyocytes (original magnification: ×400) were traced and the cardiomyocyte areas were calculated. One hundred cells per left ventricle were counted, and the averaged value was used for analysis.

Determination of cardiac fibrosis
To determine the extent of collagen fibre accumulation, paraffin slices from each heart were subjected to van Giessen-staining. Forty fields in three individual sections were selected randomly and the ratio of the areas of van Giessen-stained interstitial fibrosis to the total left ventricular area was calculated using image analysis software and a Zeiss KS400 system (Carl Zeiss Vision, Eching, Germany) (Li *et al.*, 2002; 2004).

Analysis of gene expression
Total RNA was isolated from left ventricles with the TRIzol reagent (Life Technologies Inc., Rockville, MD, USA). Expression of mRNAs encoding ANP and collagen I was evaluated using real-time RT-PCR in an ABI PRISM™ 7700 Sequence Detector (Applied Biosystems, Foster city, CA, USA). The primers and probes of the genes examined were as follows: ANP: sense, 5′-GCCATATTGGAGCAAATCCT-3′; antisense, 5′-GCAGGTTCTTGAAATCCATCA-3′; oligonucleotide probe, 5′-TGTACAGTGCGGTGTCCAACACAGAT-3′; collagen I: sense, 5′-GTCCCAACCCCCAAAGAC-3′; antisense, 5′-CAT

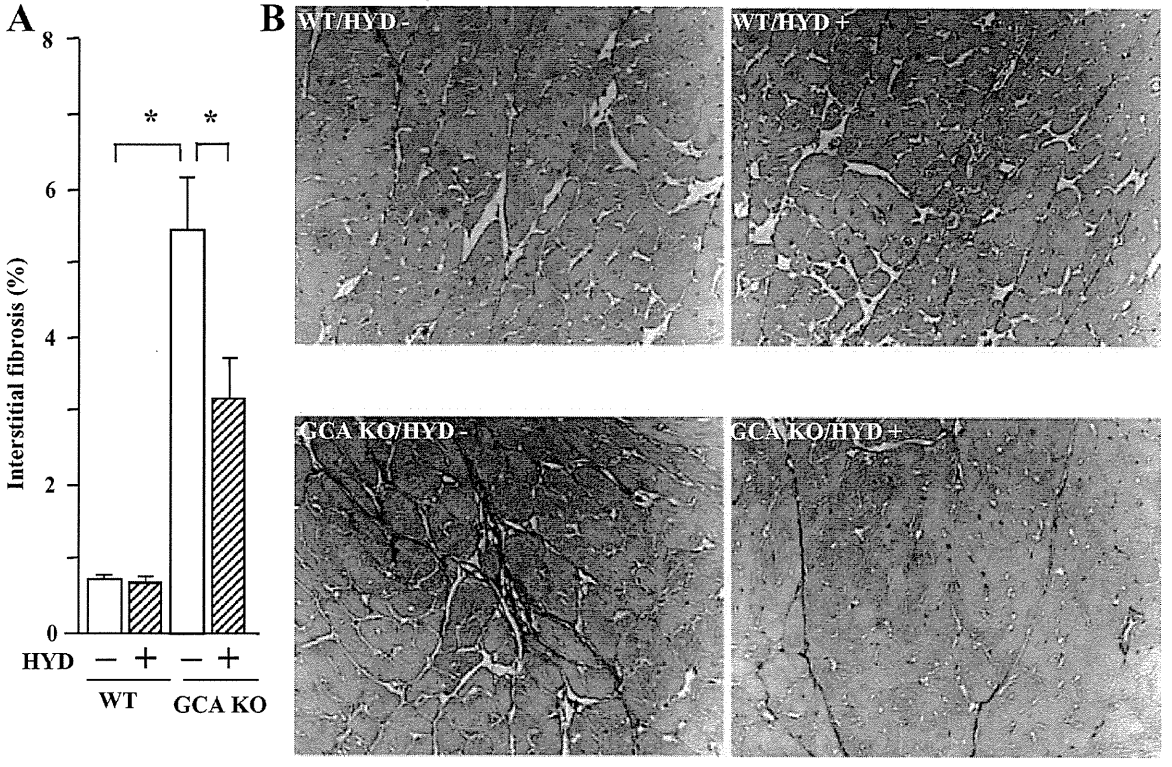

Figure 3 Cardiac fibrosis in wild-type (WT) and guanylyl cyclase-A (GCA) knockout (KO) mice. Hydralazine (HYD) was administered in drinking water (≈24 mg·kg^{-1}·day^{-1}) for 5 weeks, while the mice in control groups received drinking water only. After van Giessen-staining the area of collagen deposition in the interstitial region and the total left ventricular area were quantified using an image analysing system. (A) Interstitial fibrosis (%, the ratio of the area of interstitial collagen accumulation to the total left ventricular area); (B) Representative examples of interstitial fibrosis (red) (original magnification: ×200). Values are means ± SEM (n = 7–14). *P < 0.05. HYD –: control, without HYD; HYD +, with HYD.

CTTCTGAGTTTGGTGATACGT-3′; oligonucleotide probe, 5′-CACGGCTGTGTGCGATGACG-3′. To verify that equal amounts of mRNA were subjected to real-time RT-PCR, GAPDH mRNA was also amplified using the same method with specific primers and probe (Applied Biosystems, Hammonton, NJ, USA).

Statistical analysis

All data are expressed as means ± SEM of values obtained in individual animals. Data were analysed by single-factor ANOVA. If a significant effect was found, the Student-Newman-Keuls test was performed to isolate the difference between the groups. Values of $P < 0.05$ were considered statistically significant.

Results

HR, SBP, cardiac mass, collagen accumulation and expression of hypertrophic and fibrogenic genes in WT and GCA KO mice

The antihypertensive agent hydralazine was used to assess the role of blood pressure in the development of cardiac hypertrophy in GCA-deficient mice. HR was not different between the four groups of WT and GCA KO mice at baseline (data not shown). Consistent with enhancement of cardiac sympathetic activity (Tsoporis and Leenen, 1988), hydralazine (≈24 mg·kg^{-1}·day^{-1} in drinking water) significantly increased HR in WT and GCA KO mice over the course of the experiment, but there was no difference between the treated groups (data not shown). In contrast, SBP was increased in GCA KO mice compared with WT mice (Figure 1A). In accord with previous findings, hydralazine elicited a potent and stable antihypertensive effect in WT mice (Figure 1A). Although hydralazine also lowered SBP in GCA KO mice after 1 week of treatment, its efficacy diminished over the course of the 5 week experimental period.

Hydralazine did not alter BW in mice (WT control: 33.9 ± 1.4 g; WT + hydralazine: 32.4 ± 0.8 g; GCA KO control: 33.9 ± 2.1g; GCA KO + hydralazine: 34.4 ± 1.0 g). The HW/BW (Figure 1B) and the LVW/BW (Figure 1C) ratios were higher in GCA KO than in WT mice. The cross-sectional area of cardiac myocytes was also increased in GCA KO mice (Figure 2). Somewhat surprisingly, treatment with hydralazine over 5 weeks markedly increased the ratios of HW/BW and LVW/BW, and the cross-sectional area in GCA KO mice, but not in WT mice (Figures 1B,C and 2A).

There was a pronounced increase in cardiac interstitial van Giessen-staining area, as a measure of fibrosis, in GCA KO mice compared with WT (Figure 3). In contrast to the effect on HW/BW and LVW/BW, hydralazine selectively decreased the extent of van Giessen-staining in cardiac sections from GCA KO mice.

Consistent with the phenotypic change in cardiac mass, cardiac expression of the mRNA for ANP, an important molecular marker of cardiac hypertrophy, was greater in GCA KO mice than in WT controls (Figure 4A). The increase in cardiac ANP expression suggests that the GCA deficiency-induced cardiac hypertrophy may not be compensatory, but may be a component of a decompensation process. Hydralazine treatment further enhanced cardiac expression of mRNA for ANP in GCA KO mice, but induced no change in WT animals ($P > 0.05$). In contrast, the up-regulation of cardiac collagen I mRNA (the most important collagen isoform in heart) in GCA KO mice was suppressed by hydralazine treatment (Figure 4B). Hydralazine did not affect collagen I mRNA expression in WT mice.

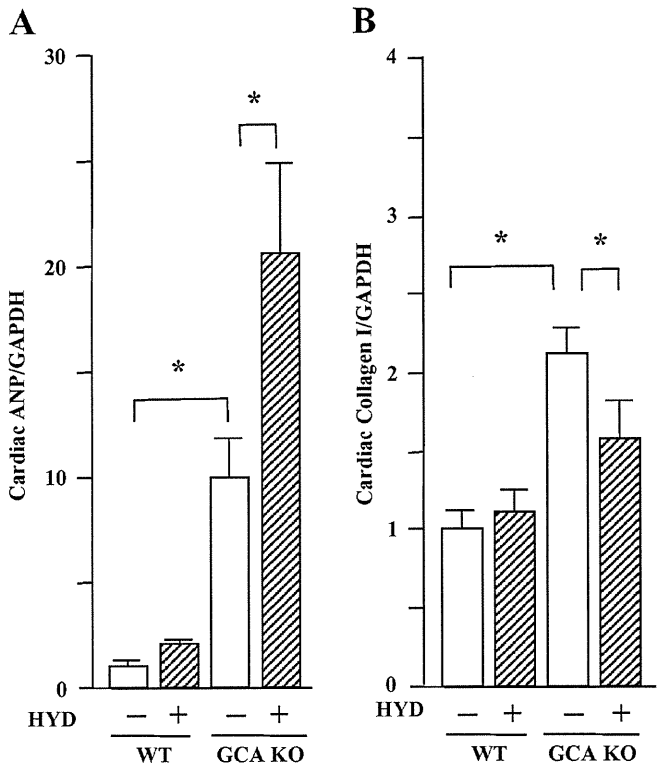

Figure 4 Left ventricular expression of mRNA for atrial natriuretic peptide (ANP, A) or collagen I (B) in wild-type (WT) and guanylyl cyclase-A (GCA) knockout (KO) mice. Hydralazine (HYD) was administered in drinking water (≈24 mg·kg^{-1}·day^{-1}) for 5 weeks, while the mice in control groups received drinking water only. Total RNA was extracted from the left ventricular tissues using TRIzol. The relative levels of specific mRNAs were assessed by real-time RT-PCR. Results were normalized to GAPDH. Levels in WT group were arbitrarily assigned a value of 1. Values are means ± SEM ($n = 7$). *$P < 0.05$. HYD –: control, without HYD; HYD +, with HYD.

HR, SBP, cardiac mass, collagen accumulation and expression of cardiac hypertrophic and fibrogenic genes in AT_1 receptor KO and in GCA and AT_1 receptor DKO mice

The potential role of AT_1 receptors in the exacerbation of cardiac hypertrophy in GCA KO mice by hydralazine was assessed. As found in WT and GCA KO mice, there was no difference in basal HR between the four groups of AT_1 receptor KO and GCA/AT_1 DKO mice (data not shown). Hydralazine significantly increased HR in AT_1 KO and GCA/AT_1 DKO mice over the experimental time course, but there was no difference between the treated groups (data not shown). SBP was considerably lower in untreated AT_1 KO and GCA/AT_1 DKO mice (Figure 5A) than in corresponding WT and GCA KO mice (Figure 1A) respectively. However, basal SBP in GCA/AT_1

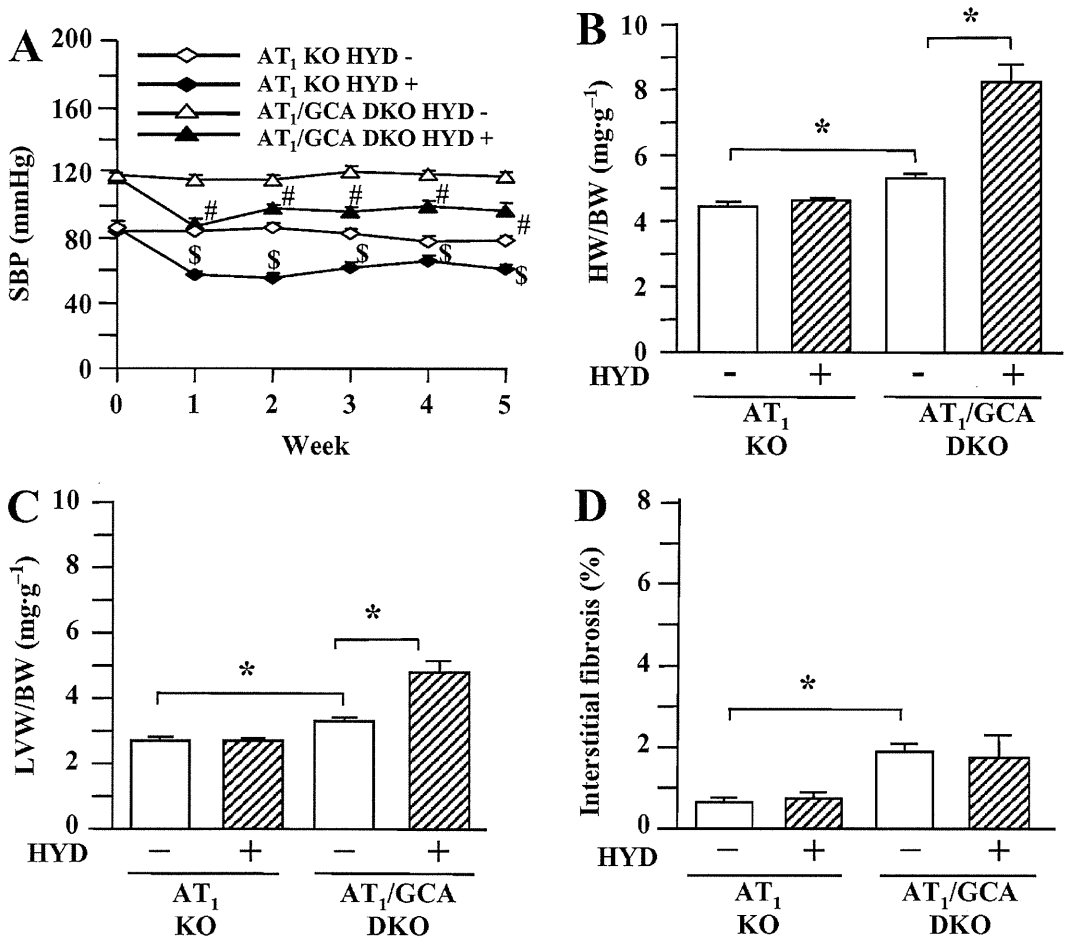

Figure 5 Systolic blood pressure (SBP, A), the ratios of heart weight to body weight (HW/BW, B) and left ventricular weight to body weight (LVW/BW, C) and cardiac interstitial fibrosis (D) in angiotensin II type 1 (AT_1) receptor knockout (KO) and guanylyl cyclase-A (GCA)/AT_1 double KO (DKO) mice. Hydralazine (HYD) was administered in drinking water (≈24 $mg \cdot kg^{-1} \cdot day^{-1}$) for 5 weeks, while the mice in control groups received drinking water only. SBP was measured in conscious mice prior to, and at weekly intervals after, the commencement of treatment using a computerized tail-cuff method. Hearts and left ventricles were weighed at the conclusion of the experiments (week 5), and HW/BW and LVW/BW were calculated. After van Giessen-staining the area of collagen deposition on the interstitial region and the total left ventricular area were quantified using an image analysing system. Values are means ± SEM ($n = 6–7$). *$P < 0.05$; $^{\$}$different from AT_1 KO (HYD –), or $^{\#}$different from GCA/AT_1 DKO (HYD –) at corresponding time-points ($P < 0.05$). HYD –: control, without HYD; HYD +, with HYD.

DKO mice was still higher than that in AT_1 KO mice. Hydralazine treatment further decreased SBP in both AT_1 KO and AT_1/GCA DKO mice.

Hydralazine treatment was without effect on BW in both genotypes (AT_1 receptor KO control: 36.0 ± 1.3 g; AT_1 KO + hydralazine: 35.3 ± 1.0 g; GCA/AT_1 DKO control: 36.1 ± 1.3 g; GCA/AT_1 DKO + hydralazine: 36.6 ± 1.5 g). Further, HW/BW (Figure 5B) and LVW/BW ratios (Figure 5C), as well as cardiac ANP mRNA expression (Figure 6A), were lower in untreated AT_1 KO and GCA/AT_1 DKO mice than untreated WT and GCA KO mice (Figures 1B,C and 4A). Hydralazine increased the HW/BW and LVW/BW ratios (Figure 5B,C) and cardiac ANP mRNA expression (Figure 6A) in GCA/AT_1 DKO mice, whereas this treatment was without effect on these parameters in AT_1 receptor KO mice.

Deletion of AT_1 receptors decreased the extent of van Giessen-staining in cardiac interstitial sections from more than 5% (Figure 3A) to less than 2% (Figure 5D) and also decreased collagen I mRNA expression (Figure 6B) in GCA KO mice, compared with basal conditions. Hydralazine treatment did not affect residual cardiac fibrosis, collagen I mRNA expression or these parameters in AT_1 KO mice (Figures 5D and 6B).

HR, SBP, cardiac mass, collagen accumulation and cardiac gene expression of hypertrophic and fibrogenic markers in AT_2 receptor KO and GCA and in AT_2 DKO mice

The potential role of AT_2 receptors in hydralazine-induced exacerbation of the cardiac hypertrophy observed in GCA KO mice was also assessed in the present study. As we had observed in WT, GCA KO, AT_1 KO and GCA/AT_1 DKO mice, there was no difference in basal HR in four groups of AT_2 receptor KO and GCA/AT_2 DKO mice (data not shown). Hydralazine significantly increased HR in AT_2 KO and GCA/AT_2 DKO mice over the course of the experiment, but there was no difference between the treated groups (data not shown). Deletion of AT_2 receptors did not affect SBP

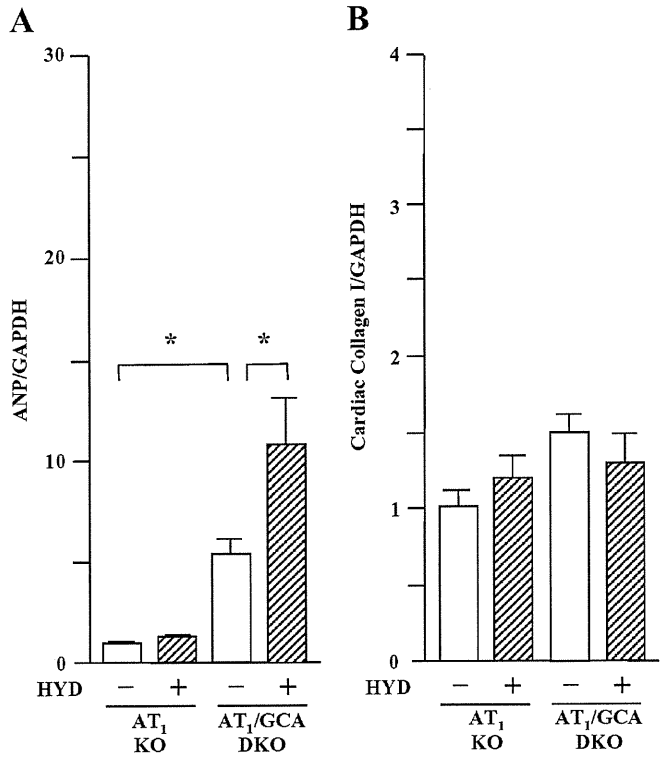

Figure 6 Left ventricular expression of mRNA for atrial natriuretic peptide (ANP, A) and collagen I (B) in angiotensin II type 1 (AT_1) receptor knockout (KO) and guanylyl cyclase-A (GCA)/AT_1 double KO (DKO) mice. Hydralazine (HYD) was administered in drinking water (≈24 $mg \cdot kg^{-1} \cdot day^{-1}$) for 5 weeks, while the mice in control groups received drinking water only. Total RNA was extracted from the left ventricular tissues using TRIzol. The relative levels of specific mRNAs were assessed by real-time RT-PCR. Results were normalized to GAPDH. Levels in WT group were arbitrarily assigned a value of 1. Values are means ± SEM ($n = 6–7$). *$P < 0.05$. HYD −: control, without HYD; HYD +, with HYD.

(Figure 7A), compared with corresponding animals that expressed AT_2 (Figure 1A). Hydralazine decreased SBP in both AT_2 KO and AT_2/GCA DKO mice (Figure 7A) but was without effect on BW (AT_2 KO control: 34.0 ± 1.3 g; AT_2 KO + hydralazine: 36.2 ± 1.5 g; GCA/AT_2 DKO control: 35.1 ± 1.1 g; GCA/AT_2 DKO + hydralazine: 36.0 ± 1.3 g). Unlike the situation in GCA KO and GCA/ AT_1 DKO mice, hydralazine treatment had no effect on the HW/BW (Figure 7B) and LVW/BW (Figure 7C) ratios. The cardiac ANP mRNA expression (Figure 8A) was not changed by hydralazine in AT_2 receptor KO but suppressed in GCA/AT_2 DKO mice.

In contrast to the effects in GCA KO mice (Figure 3A), cardiac van Giessen-staining was decreased in GCA/AT_2 DKO animals (Figure 7D). Hydralazine treatment further decreased cardiac interstitial fibrosis in GCA/AT_2 DKO mice, but did not affect collagen deposition in AT_2 receptor KO mouse heart (Figure 7D) or collagen I mRNA expression in both genotypes ($P > 0.05$) (Figure 8B).

Discussion

The present results clearly demonstrated that hydralazine increased the HW/BW and LVW/BW ratios, cardiomyocyte cross-sectional area and cardiac ANP mRNA in mice lacking GCA, but not in WT mice, despite its antihypertensive actions. Thus, vasodilator therapy augmented cardiac hypertrophy under conditions of GCA deficiency. Long-term treatment with hydralazine in rats or humans is known to increase plasma renin activity (Tsoporis and Leenen, 1986; Leenen *et al.*, 1987) and induces cardiac sympathetic hyperactivity (Tsoporis and Leenen, 1988), as well as cardiac volume overload (Tsoporis *et al.*, 1989). However, the molecular mechanisms underlying the pro-hypertrophic actions of hydralazine are presently unclear.

It is well established that angiotensin II plays an important role in the development of cardiac hypertrophy, and that AT_1 receptors mediate most of the known physiological effects of angiotensin II (Hunyady and Turu, 2004). Hydralazine has been reported to increase plasma renin activity in spontaneously hypertensive rats (Tsoporis and Leenen, 1986; 1988). We have demonstrated previously that genetic or pharmacological blockade of AT_1 receptors attenuated cardiac hypertrophy in GCA KO mice (Li *et al.*, 2002) and that AT_1 receptors were responsible for hypertrophy induced in GCA KO mouse heart by androgens (Li *et al.*, 2004). We initially speculated that angiotensin II/AT_1 receptor signalling might participate in hydralazine-induced cardiac growth. Somewhat unexpectedly, however, hydralazine treatment increased cardiac mass and enhanced cardiac expression of the hypertrophic marker ANP in GCA/AT_1 DKO mice, but not in mice lacking AT_1 receptors alone. Thus, the present findings suggest that hydralazine-induced pro-hypertrophic signalling was independent of AT_1 receptors. On the other hand, the persistence of the antihypertensive actions of hydralazine in the GCA/AT_1 receptor DKO mice supports the contention that cardiac hypertrophy was independent of blood pressure in these animals.

The AT_2 receptor is the other major angiotensin II receptor subtype. Its expression is up-regulated in cardiovascular pathologies, including cardiac hypertrophy (Suzuki *et al.*, 1993; Lopez *et al.*, 1994) and heart failure (Tsutsumi *et al.*, 1998). Although the role of AT_2 receptors in cardiac remodelling remains controversial, accumulating lines of evidence appear to support the view that AT_2 receptors can promote cardiac growth in certain pathological situations. Indeed, at least in some tissues, AT_1 and AT_2 receptors share common signalling pathways that stimulate cell and tissue proliferation (Mifune *et al.*, 2000; Senbonmatsu *et al.*, 2000; Ichihara *et al.*, 2001; Yan *et al.*, 2003; D'Amore *et al.*, 2005). We have recently demonstrated that expression of AT_2 receptors at the mRNA and protein level is up-regulated in hearts of GCA KO mice and that both genetic and pharmacological blockade of AT_2 receptors ameliorated the cardiac hypertrophy induced by GCA deficiency (Li *et al.*, 2009). The pro-hypertrophic effect of hydralazine observed in GCA KO and GCA/AT_1 DKO mice was completely abolished in GCA/AT_2 DKO animals, and hydralazine treatment also decreased cardiac mass and ANP gene expression. These results suggest that hydralazine-induced pro-hypertrophic signalling in the heart was dependent on AT_2 receptors.

The other finding in the present study is that hydralazine treatment attenuates cardiac fibrosis in GCA KO mice. It is generally considered that there are two types of cardiac

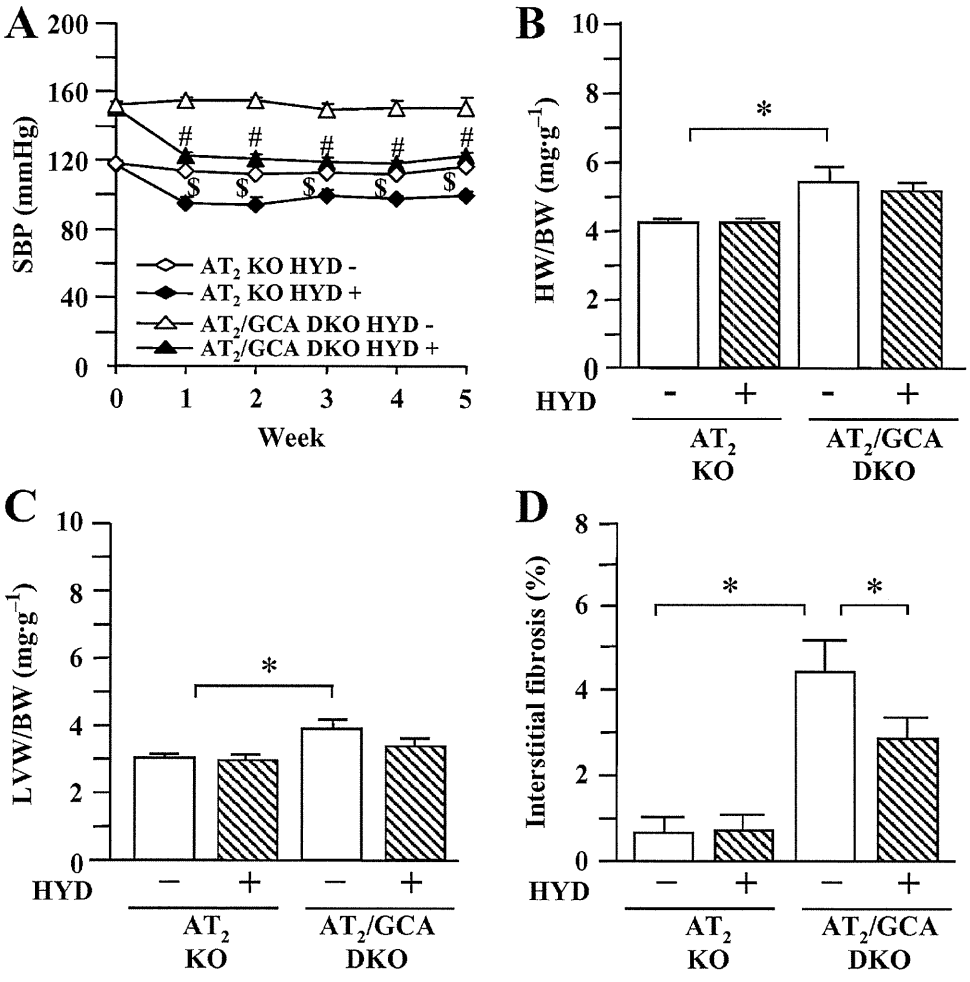

Figure 7 Systolic blood pressure (SBP, A), the ratios of heart weight to body weight (HW/BW, B) and left ventricular weight to body weight (LVW/BW, C) and cardiac interstitial fibrosis (D) in angiotensin II type 2 (AT_2) receptor knockout (KO) and guanylyl cyclase-A (GCA)/AT_2 double KO (DKO) mice. Hydralazine (HYD) was administered in drinking water (≈24 $mg \cdot kg^{-1} \cdot day^{-1}$) for 5 weeks, while the mice in control groups received drinking water only. SBP was measured in conscious mice prior to, and at weekly intervals after, the commencement of treatment using a computerized tail-cuff method. Hearts and left ventricles were weighed at the conclusion of the experiments (week 5), and HW/BW and LVW/BW were calculated. After van Giessen-staining the area of collagen deposition on the interstitial region and the total left ventricular area were quantified using an image analysing system. Values are means ± SEM ($n = 7–8$). *$P < 0.05$; $^{\$}$different from AT_2 KO (HYD –), or $^{\#}$different from GCA/AT_2 DKO (HYD –) at corresponding time-points ($P < 0.05$). HYD –: control, without HYD; HYD +, with HYD.

fibrosis: reparative and reactive fibrosis. Reparative fibrosis appears to be a reaction to the loss of myocardial material (due to necrosis or apoptosis, after myocardial ischemia or senescence) and is primarily interstitial in location. In contrast, reactive fibrosis is observed in the absence of cell loss and appears to be a reaction to inflammation; it is primarily located perivascularly (Swynghedauw, 1999). Hydralazine therapy has previously been found to be ineffective in the modification of reactive fibrosis (Mukherjee and Sen, 1993; Norton *et al.*, 1997). In contrast, hydralazine treatment prevented the development of reparative fibrosis in spontaneously hypertensive rats (Tsotetsi *et al.*, 2001). In addition, hydralazine has been shown to inhibit prolyl hydroxylase activity (Bhatnagar *et al.*, 1972; Knowles *et al.*, 2004), which prevents the post-translational modification of collagen prolyl residues essential for the formation of stable collagen fibres (Murad *et al.*, 1985). In the present study, even though hydralazine promoted the growth of cardiomyocytes, the same treatment diminished cardiac interstitial fibrosis in GCA KO mice. This suggests that there may be different mechanisms by which the growth of cardiomyocytes and cardiac fibroblasts is regulated in GCA-deficient mice. Future studies are required to address whether myocardial ischaemia and/or prolyl hydroxylase overactivity are associated with the excessive cardiac collagen accumulation in GCA deficiency.

In conclusion, the present findings indicate that vasodilator therapy with hydralazine induces AT_2 receptor-dependent, but AT_1 receptor-independent, growth of cardiomyocytes in mice lacking GCA. Thus, the possibility that exacerbation of cardiac hypertrophy may occur during the use of hydralazine in patients with decreased GCA activity should now be considered. On the other hand, attenuation of cardiac fibrosis by hydralazine treatment could be beneficial in the management of cardiac disease. The precise mechanisms underlying the anti-fibrotic action of hydralazine should now be addressed further.

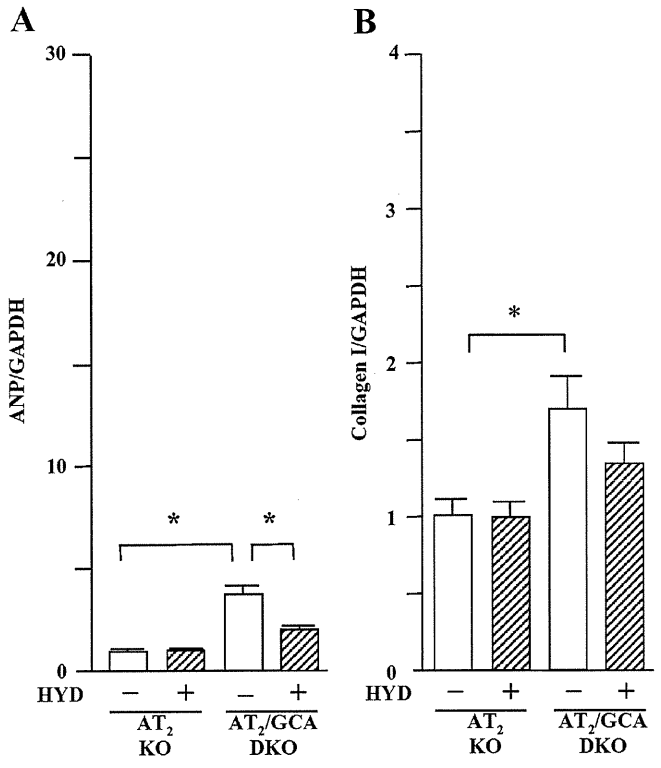

Figure 8 Left ventricular expression of mRNA for atrial natriuretic peptide (ANP, A) and collagen I (B) in angiotensin II type 2 (AT_2) receptor and in guanylyl cyclase-A (GCA) and AT_2 double knockout (DKO) mice. Hydralazine (HYD) was administered in drinking water (≈24 $mg \cdot kg^{-1} \cdot day^{-1}$) for 5 weeks, while the mice in control groups received drinking water only. Total RNA was extracted from the left ventricular tissues using TRIzol. The relative levels of specific mRNAs were assessed by real-time RT-PCR. Results were normalized to GAPDH. Levels in wild-type group were arbitrarily assigned a value of 1. Values are means ± SEM ($n = 7–8$). *$P < 0.05$. HYD –: control, without HYD; HYD +, with HYD.

Acknowledgements

This work was supported in partly by research grants from the Japanese Ministry of Education, Science and Culture, the Japanese Ministry of Health and Welfare and the Japanese Society for the Promotion of Science, Japan.

Statement of conflicts of interest

None.

References

Bauer JA, Fung HL (1991). Concurrent hydralazine administration prevents nitroglycerin-induced hemodynamic tolerance in experimental heart failure. *Circulation* **84**: 35–39.

Bhatnagar RS, Rapaka SSR, Liu TZ, Wolfe SM (1972). Hydralazine-induced disturbances in collagen biosynthesis. *Biochim Biophys Acta* **271**: 125–132.

D'Amore A, Black MJ, Thomas WG (2005). The angiotensin II type 2 receptor causes constitutive growth of cardiomyocytes and does not antagonize angiotensin II type 1 receptor-mediated hypertrophy. *Hypertension* **46**: 1347–1354.

Fenje P, Leenen FH (1985). Effects of minoxidil on blood pressure and cardiac hypertrophy in two-kidney, one-clip hypertensive rats. *Can J Physiol Pharmacol* **63**: 161–164.

Gerber JG, Nies AS (1990). Ahtihypertensive agents and the drug therapy of hypertension. In: Gilman AG, Rall TW, Nies AS, Taylor P (eds). *The Pharmacological Basis of Therapeutics*. Pergamon Press: New York, pp. 784–813.

Gogia H, Mehra A, Parikh S, Raman M, Ajit-Uppal J, Johnson JV *et al.* (1995). Prevention of tolerance to hemodynamic effects of nitrates with concomitant use of hydralazine in patients with chronic heart failure. *J Am Coll Cardiol* **26**: 1575–1580.

Heart Failure Society of America (2006). Executive summary: HFSA 2006 Comprehensive Heart Failure Practice Guideline. *J Card Fail* **12**: 10–38.

Hunt SA, Abraham WT, Chin MH, Feldman AM, Francis GS, Ganiats TG *et al.* (2005). American Heart Association Task Force on Practice Guidelines; American College of Chest Physicians; International Society for Heart and Lung Transplantation; Heart Rhythm Society. ACC/AHA 2005 guideline update for the diagnosis and management of chronic heart failure in the adult. *Circulation* **112**: e154–e235.

Hunt SA, Abraham WT, Chin MH, Feldman AM, Francis GS, Ganiats TG *et al.* (2009a). 2009 focused update incorporated into the ACC/AHA 2005 Guidelines for the Diagnosis and Management of Heart Failure in Adults: a report of the American College of Cardiology Foundation/American Heart Association Task Force on Practice Guidelines: developed in collaboration with the International Society for Heart and Lung Transplantation. *Circulation* **119**: e391–e479.

Hunt SA, Abraham WT, Chin MH, Feldman AM, Francis GS, Ganiats TG *et al.* (2009b). 2009 focused update incorporated into the ACC/AHA 2005 Guidelines for the Diagnosis and Management of Heart Failure in Adults: a report of the American College of Cardiology Foundation/American Heart Association Task Force on Practice Guidelines: developed in collaboration with the International Society for Heart and Lung Transplantation. *J Am Coll Cardiol* **53**: e1–e90.

Hunyady L, Turu G (2004). The role of the AT1 angiotensin receptor in cardiac hypertrophy: angiotensin II receptor or stretch sensor? *Trends Endocrinol Metab* **15**: 405–408.

Ichihara S, Senbonmatsu T, Price E Jr, Ichiki T, Gaffney FA, Inagami T (2001). Angiotensin type 2 receptor is essential for ventricular hypertrophy and cardiac fibrosis in chronic angiotensin II-induced hypertension. *Circulation* **104**: 346–351.

Kleaveland JP, Reichek N, McCarthy DM, Chandler T, Priest C, Muhammed A *et al.* (1986). Effects of six-month afterload reduction therapy with hydralazine in chronic aortic regurgitation. *Am J Cardiol* **57**: 1109–1116.

Knowles HJ, Tian YM, Mole DR, Harris AL (2004). Novel mechanism of action for hydralazine: induction of hypoxia-inducible factor-1alpha, vascular endothelial growth factor, and angiogenesis by inhibition of prolyl hydroxylases. *Circ Res* **95**: 162–169.

Leenen FH, Prowse S (1987). Time-course of changes in cardiac hypertrophy and pressor mechanisms in two-kidney, one-clip hypertensive rats during treatment with minoxidil, enalapril or after uninephrectomy. *J Hypertens* **5**: 73–83.

Leenen FH, Smith DL, Farkas RM, Reeves RA, Marquez-Julio A (1987). Vasodilators and regression of left ventricular hypertrophy. Hydralazine versus prazosin in hypertensive humans. *Am J Med* **82**: 969–978.

Li Y, Kishimoto I, Saito Y, Harada M, Kuwahara K, Izumi T *et al.* (2002). Guanylyl cyclase A inhibits angiotensin II type 1a receptor-mediated cardiac remodeling, an endogenous protective mechanism in the heart. *Circulation* **106**: 1722–1728.

Li Y, Kishimoto I, Saito Y, Harada M, Kuwahara K, Izumi T *et al.* (2004). Androgen contributes to gender-related cardiac

hypertrophy and fibrosis in mice lacking the gene encoding guanylyl cyclase-A. *Endocrinology* **145**: 951–958.

Li Y, Saito Y, Kuwahara K, Rong X, Kishimoto I, Harada M *et al.* (2009). Guanylyl cyclase-A inhibits angiotensin II type 2 receptor-mediated pro-hypertrophic signaling in the heart. *Endocrinology* **150**: 3759–3765.

Lopez JJ, Lorell BH, Ingefinger JR, Weinberg EO, Schunkert H, Diamant D *et al.* (1994). Distribution and function of cardiac angiotensin AT1- and AT2-receptor subtypes in hypertrophied rat hearts. *AM J Physiol* **267**: H844–H852.

Lopez MJ, Wong SKF, Kishimoto I, Dubois S, Mach V, Friesen J *et al.* (1995). Salt-resistant hypertension in mice lacking the guanylyl cyclase-A receptor for atrial natriuretic peptide. *Nature* **378**: 65–68.

Mifune M, Sasamura H, Shimizu-Hirota R, Miyazaki H, Saruta T (2000). Angiotensin II type 2 receptors stimulate collagen synthesis in cultured vascular smooth muscle cells. *Hypertension* **36**: 845–850.

Mukherjee D, Sen S (1993). Alteration of collagen phenotypes in hypertensive hypertrophy: role of blood pressure. *J Mol Cell Cardiol* **25**: 185–196.

Murad S, Tajima S, Pinnell SR (1985). A paradoxical effect of hydralazine on prolyl and lysyl hydroxylase activities in cultured human skin fibroblasts. *Arch Biochem Biophys* **241**: 356–363.

Nakanishi M, Saito Y, Kishimoto I, Harada M, Kuwahara K, Takahashi N *et al.* (2005). Role of natriuretic peptide receptor GC-A in myocardial infarction evaluated using genetically engineered mice. *Hypertension* **46**: 441–447.

Nakayama T, Soma M, Takahashi Y, Rehemudula D, Kanmatsuse K, Furuya K (2000). Functional deletion mutation of the 5′-flanking region of type A human natriuretic peptide receptor gene and its association with essential hypertension and left ventricular hypertrophy in the Japanese. *Circ Res* **86**: 841–845.

Norton GR, Tsotetsi J, Trifunovic B, Hartford C, Candy GP, Woodiwiss AJ (1997). Myocardial stiffness is attributed to alterations in cross-linked rather than total collagen or phenotypes in spontaneously hypertensive rats. *Circulation* **96**: 1991–1998.

Oliver PM, Fox JE, Kim R, Rockman HA, Kim HS, Reddick RL *et al.* (1997). Hypertension, cardiac hypertrophy, and sudden death in mice lacking natriuretic peptide receptor A. *Proc Natl Acad Sci USA* **94**: 14731–14735.

Pegram BL, Ischise S, Frolich ED (1982). Effect of methyldopa, clonidine, and hydralazine on cardiac mass and haemodynamicsin Wistar-Kyoto and SHR. *Cardiovasc Res* **16**: 40–46.

Rubattu S, Bigatti G, Evangelista A, Lanzani C, Stanzione R, Zagato L *et al.* (2006). Association of atrial natriuretic peptide and type a natriuretic peptide receptor gene polymorphisms with left ventricular mass in human essential hypertension. *J Am Coll Cardiol* **48**: 499–505.

Sanada S, Node K, Minamino T, Takashima S, Ogai A, Asanuma H *et al.* (2003). Long-acting Ca^{2+} blockers prevent myocardial remodeling induced by chronic NO inhibition in rats. *Hypertension* **41**: 963–967.

Sen S, Tarazi RC, Bumpus FM (1974). Cardiac hypertrophy in SHR. *Circ Res* **35**: 775–781.

Sen S, Tarazi RC, Bumpus FM (1977). Cardiac hypertrophy and antihypertensive therapy. *Cardiovasc Res* **11**: 427–433.

Senbonmatsu T, Ichihara S, Price E Jr, Gaffney FA, Inagami T (2000). Evidence for angiotensin II type 2 receptor-mediated cardiac myocyte enlargement during *in vivo* pressure overload. *J Clin Invest* **106**: R25–R29.

Suzuki J, Matsubara H, Urakami M, Inada M (1993). Rat angiotensin II (type 1A) receptor mRNA regulation and subtype expression in myocardial growth and hypertrophy. *Cir Res* **73**: 439–447.

Swynghedauw B (1999). Molecular mechanisms of myocardial remodeling. *Physiol Rev* **79**: 215–262.

Taylor AL, Ziesche S, Yancy C, Carson P, D'Agostino R Jr, Ferdinand K *et al.* (2004). Combination of isosorbide dinitrate and hydralazine in blacks with heart failure. *N Engl J Med* **351**: 2049–2057.

Tsoporis J, Leenen FH (1986). Effects of hydralazine on blood pressure, pressor mechanisms and cardiac hypertrophy in twokidney, one-clip hypertensive rats. *Can J Physiol Pharmacol* **64**: 1528–1534.

Tsoporis J, Leenen FH (1988). Effects of arterial vasodilators on cardiac hypertrophy and sympathetic activity in rats. *Hypertension* **11**: 376–386.

Tsoporis J, Yuan BX, Leenen FH (1989). Arterial vasodilators, cardiac volume load, and cardiac hypertrophy in normotensive rats. *Am J Physiol* **256** (3 Pt 2): H876–H880.

Tsotetsi OJ, Woodiwiss AJ, Netjhardt M, Qubu D, Brooksbank R, Norton GR (2001). Attenuation of cardiac failure, dilatation, damage, and detrimental interstitial remodeling without regression of hypertrophy in hypertensive rats. *Hypertension* **38**: 846–851.

Tsutamoto T, Kanamori T, Wada A, Kinoshita M (1992). Uncoupling of atrial natriuretic peptide extraction and cyclic guanosine monophosphate production in the pulmonary circulation in patients with severe heart failure. *J Am Coll Cardiol* **20**: 541–546.

Tsutamoto T, Kanamori T, Morigami N, Sugimoto Y, Yamaoka O, Kinoshita M (1993). Possibility of downregulation of atrial natriuretic peptide receptor coupled to guanylate cyclase in peripheral vascular beds of patients with chronic severe heart failure. *Circulation* **87**: 70–75.

Tsutsumi Y, Matsubara H, Ohkubo N, Mori Y, Nozawa Y, Murasawa S *et al.* (1998). Angiotensin II type 2 receptor is upregulated in human heart with interstitial fibrosis, and cardiac fibroblasts are the major cell type for its expression. *Cir Res* **83**: 1035–1046.

Usami S, Kishimoto I, Saito Y, Harada M, Kuwahara K, Nakagawa Y *et al.* (2008). Association of CT dinucleotide repeat polymorphism in the 5′-flanking region of the guanylyl cyclase (GC)-A gene with essential hypertension in the Japanese. *Hypertens Res* **31**: 89–96.

Yan X, Price RL, Nakayama M, Ito K, Schuldt AJ, Manning WJ *et al.* (2003). Ventricular-specific expression of angiotensin II type 2 receptors causes dilated cardiomyopathy and heart failure in transgenic mice. *Am J Physiol Heart Circ Physiol* **285**: H2179–H2187.

Am J Physiol Endocrinol Metab 298: E930–E940, 2010.
First published September 23, 2009; doi:10.1152/ajpendo.00320.2009.

Glucocorticoid reamplification within cells intensifies NF-κB and MAPK signaling and reinforces inflammation in activated preadipocytes

Takako Ishii-Yonemoto, Hiroaki Masuzaki, Shintaro Yasue, Sadanori Okada, Chisayo Kozuka, Tomohiro Tanaka, Michio Noguchi, Tsutomu Tomita, Junji Fujikura, Yuji Yamamoto, Ken Ebihara, Kiminori Hosoda, and Kazuwa Nakao

Division of Endocrinology and Metabolism, Department of Medicine and Clinical Science, Kyoto University Graduate School of Medicine, Sakyoku, Japan

Submitted 18 May 2009; accepted in final form 16 September 2009

Ishii-Yonemoto T, Masuzaki H, Yasue S, Okada S, Kozuka C, Tanaka T, Noguchi M, Tomita T, Fujikura J, Yamamoto Y, Ebihara K, Hosoda K, Nakao K. Glucocorticoid reamplification within cells intensifies NF-κB and MAPK signaling and reinforces inflammation in activated preadipocytes. *Am J Physiol Endocrinol Metab* 298: E930–E940, 2010. First published September 23, 2009; doi:10.1152/ajpendo.00320.2009.—Increased expression and activity of the intracellular glucocorticoid-reactivating enzyme 11β-hydroxysteroid dehydrogenase type 1 (11β-HSD1) contribute to dysfunction of adipose tissue. Although the pathophysiological role of 11β-HSD1 in mature adipocytes has long been investigated, its potential role in preadipocytes still remains obscure. The present study demonstrates that the expression of 11β-HSD1 in preadipocyte-rich stromal vascular fraction (SVF) cells in fat depots from *ob/ob* and diet-induced obese mice was markedly elevated compared with lean control. In 3T3-L1 preadipocytes, the level of mRNA and reductase activity of 11β-HSD1 was augmented by TNF-α, IL-1β, and LPS, with a concomitant increase in inducible nitric oxide synthase (iNOS), monocyte chemoattractant protein-1 (MCP-1), or IL-6 secretion. Pharmacological inhibition of 11β-HSD1 and RNA interference against 11β-HSD1 reduced the mRNA and protein levels of iNOS, MCP-1, and IL-6. In contrast, overexpression of 11β-HSD1 further augmented TNF-α-induced iNOS, IL-6, and MCP-1 expression. Moreover, 11β-HSD1 inhibitors attenuated TNF-α-induced phosphorylation of NF-κB p65 and p38-, JNK-, and ERK1/2-MAPK. Collectively, the present study provides novel evidence that inflammatory stimuli-induced 11β-HSD1 in activated preadipocytes intensifies NF-κB and MAPK signaling pathways and results in further induction of proinflammatory molecules. Not limited to 3T3-L1 preadipocytes, we also demonstrated that the notion was reproducible in the primary SVF cells from obese mice. These findings highlight an unexpected, proinflammatory role of reamplified glucocorticoids within preadipocytes in obese adipose tissue.

11β-hydroxysteroid dehydrogenase type 1; preadipocyte; nuclear factor-κB; mitogen-activated protein kinase; adipose inflammation

OBESE ADIPOSE TISSUE IS CHARACTERIZED by low-grade, chronic inflammation (24, 58). In humans and rodents, it has been shown that intracellular glucocorticoid reactivation is exaggerated in obese adipose tissue (38). Two isoenzymes, 11β-hydroxysteroid dehydrogenase type 1 (11β-HSD1) and type 2 (11β-HSD2), catalyze interconversion between hormonally active cortisol and inactive cortisone (2). In particular, 11β-HSD1 is abundantly expressed in adipose tissue and preferentially reactivates cortisol from cortisone (2). In contrast, 11β-HSD2 inactivates cortisol mainly in tissues involved in water and electrolyte metabolism (60). Transgenic mice overexpressing 11β-HSD1 in adipose tissue display a cluster of fuel dyshomeostasis (61). Conversely, systemic 11β-HSD1 knockouts and adipose-specific 11β-HSD2 overexpressors, which mimic adipose-specific 11β-HSD1 knockouts, are completely protected against diabetes and dyslipidemia on a high-fat diet (14, 30, 31, 42). Interestingly, 11β-HSD1 knockout mice on a high-fat diet showed preferential accumulation of subcutaneous adipose tissue, whereas wild-type mice accumulated considerable fat pads also in visceral (mesenteric) adipose tissue (39). These findings suggest that increased activity of 11β-HSD1 in adipose tissue contributes to dysfunction of adipose tissue and subsequent metabolic derangement.

Adipose tissue is composed of mature adipocytes (~50–70% of total cells), preadipocytes (~20–40%), macrophages (~1–30%), and other cell types (22). Biopsy studies of human adipose tissue demonstrated that the distribution of adipocyte diameter is bimodal, consisting of populations of very small adipocytes ("differentiating preadipocytes") and mature adipocytes (28, 35). Interestingly, the proportion of very small adipocytes was higher in obese people compared with the lean controls (28). Notably, insulin resistance was associated with an expanded population of small adipocytes and decreased expression of differentiation marker genes, suggesting that impairment of adipocyte differentiation may contribute to obesity-associated insulin resistance (35). In this context, a potential link between preadipocyte function and pathophysiology of obese adipose tissue has recently attracted research interest (53, 57).

Many of the genes overexpressed in mature adipocytes are associated with metabolic and secretory function, whereas the most representative function of the genes overexpressed in nonmature adipocytes, i.e., stromal vascular fraction (SVF) cells, is related to inflammation and immune response (9). Macrophage infiltration into obese adipose tissue contributes to local and systemic inflammation in subjects with obesity (63, 65). Furthermore, recent research (12, 48) highlights a pathophysiological role of preadipocytes in obese adipose tissue. In the proinflammatory milieu, preadipocytes act as macrophages (11, 13), share in phagocytic activities (11), and secrete an array of inflammatory substances (13).

A pharmacological dose of glucocorticoids is widely used for anti-inflammatory therapies in human clinics (49). On the other hand, recent research is highlighting the stimulatory effects of glucocorticoids on inflammatory response. Such effects are observed at lower concentrations relevant to phys-

Address for reprint requests and other correspondence: H. Masuzaki, Division of Endocrinology and Metabolism, Dept. of Medicine and Clinical Science, Kyoto University Graduate School of Medicine, 54, Shogoin Kawaharacho, Sakyoku, Kyoto, 606-8507, Japan (e-mail: hiroaki@kuhp.kyoto-u.ac.jp).

iological stress in vivo (35, 55, 66). Therefore, the potential role of 11β-HSD1 in a variety of inflammatory responses has stimulated academic interest (10, 26). Furthermore, it is known that mature adipocytes abundantly express 11β-HSD1, which is related to adipocyte dysfunction in obese adipose tissue (44, 61). On the other hand, the role of 11β-HSD1 in SVF cells remains largely unclear.

In this context, the present study was designed to explore the expression, regulation, and pathophysiological role of 11β-HSD1 in activated preadipocytes. The results demonstrate that inflammatory stimuli-induced 11β-HSD1 reinforces NF-κB and MAPK signals and results in induction of proinflammatory molecules.

MATERIALS AND METHODS

Reagents and chemicals. All reagents were of analytical grade unless otherwise indicated. TNF-α, IL-1β, LPS, and carbenoxolone (3, 52), a nonselective inhibitor for 11β-HSD1 and 11β-HSD2, were obtained from Sigma-Aldrich (St. Louis, MO). The recently developed 11β-HSD1 selective inhibitors 3-(1-adamantyl)-5,6,7,8,9,10-hexahydro[1,2,4]triazolo[4,3-α]azocine trifluoroacetate salt (WO03/065983, inhibitor A; Merck, Whitehouse Station, NJ; Ref. 23) and 2,4,6-trichloro-*N*-(5,5-dimethyl-7-oxo-4,5,6,7-tetrahydro-1,3-benzothiazol-2-yl) benzenesulfonamide (BVT-3498; Biovitrum, Stockholm, Sweden; Ref. 25) were synthesized according to the patent information.

Polyclonal antibodies against NF-κB p65, phospho-p65, p38 MAPK, phospho-p38, ERK1/2, phospho-ERK1/2, JNK, phospho-JNK, Akt, and phospho-Akt were purchased from Cell Signaling Technology (Beverly, MA). Polyclonal antibodies against SHIP1, PP2A, and MKP-1 were purchased from Santa Cruz Biotechnology (Santa Cruz, CA). An antibody against β-actin was purchased from Upstate Biotechnology (Lake Placid, NY). Horseradish peroxidase-conjugated anti-mouse, anti-rat, and anti-rabbit IgG antibodies and ECL Plus Western blotting detection kits were purchased from Amersham Biosciences (Piscataway, NJ).

Cell culture. 3T3-L1 cells (kindly provided by Dr. H. Green and Dr. M. Morikawa, Harvard Medical School, Boston, MA) were maintained in DMEM containing 10% (vol/vol) calf serum at 37°C under 10% CO_2.

Animals. Seventeen-week-old male C57BL/6 and nine-week-old *ob/ob* mice were used for the experiments. Mice were maintained on a standard diet (F-2, 3.7 kcal/g, 12% of kcal from fat, source soybean; Funahashi Farm) or a high-fat diet (Research Diets D12493, 5.2 kcal/g, 60% of kcal from fat, source soybean/lard) under a 14:10-h light-dark cycle at 23°C. The high-fat diet was administered to the diet-induced obese (DIO) mice from 3 to 17 wk of age. Animals were allowed free access to food and water. All animal experiments were undertaken in accordance with the guidelines for animal experiments of the Kyoto University Animal Research Committee.

Isolation of SVF and the mature adipocyte fraction. Subcutaneous (SQ), mesenteric (Mes), and epididymal (Epi) fat deposits were chopped using fine scissors and digested with 2 mg/ml collagenase (Type VIII; Sigma-Aldrich) in DMEM for 1 h at 37°C under continuous shaking (170 rpm). Dispersed tissue was filtered through a nylon mesh with a pore size of 250 μm and centrifuged. Digested material was separated by centrifugation at 1,800 rpm for 5 min. The sedimented SVF and cell supernatant [mature adipocyte fraction (MAF)] were both washed with DMEM. For primary culture experiments, SVF cells from epididymal fat pads were plated in sixwell plates and cultured overnight in DMEM containing 10% (vol/vol) FBS at 37°C under 10% CO_2. After being rinsed with the medium three times, the cells were incubated with or without TNF-α, carbenoxolone, or inhibitor A for 24 h.

Quantitative real-time PCR. Total RNA was extracted using Trizol reagent (Invitrogen, Carlsbad, CA), and cDNA was synthesized using an iScript cDNA synthesis kit (Bio-Rad, Hercules, CA) according to the manufacturer's instruction. The sequences of probes and primers are summarized in Suppl. Table S1 (supplemental data for this article are available at the *Am J Physiol Endocrinol Metab* website). Taqman PCR was performed using an ABI Prism 7300 sequence detection system following the manufacturer's instructions (Applied Biosystems, Foster City, CA). mRNA levels were normalized to those of 18S rRNA.

11β-HSD1 enzyme activity assay. 11β-HSD1 acts as a reductase and reactivates cortisol from cortisone in viable cells (54). In certain substrates, however, such as tissue homogenates or the microsome fraction, 11β-HSD1 acts as a dehydrogenase and inactivates cortisol to cortisone (8). 11β-HSD1 reductase activity in intact cells was measured as reported previously (8). Cells were incubated for 24 h in serum-free DMEM, with the addition of 250 nM cortisone and tritium-labeled tracer [1,2-^{3}H]$_2$-cortisone (Muromachi Yakuhin, Kyoto, Japan) for reductase activity and 250 nM cortisol with [1,2,6,7-^{3}H]$_4$-cortisol (Muromachi Yakuhin) for dehydrogenase activity. Cortisol and cortisone were extracted using ethyl acetate, evaporated, resuspended in ethanol, separated using thin-layer chromatography in 95:5 chloroform/methanol, and quantified using autoradiography.

To validate inhibitory potency of compounds against 11β-HSD1 with the use of FreeStyle 293 cells transiently transfected with human 11β-HSD1, the enzyme activity assay was carried out with 20 mM Tris · HCl at pH 7.0, 50 μM NADPH, 5 μg protein of microsomal fraction, and 300 nM [^{3}H]cortisone for 2 h. The reaction was stopped by 18β-glycyrrhetinic acid. The labeled cortisol product was captured by mouse monoclonal anti-cortisol antibody, bound to scintillation proximity assay beads coated with protein A, and quantified in a scintillation counter.

ELISA. Monocyte chemoattractant protein-1 (MCP-1) and IL-6 concentrations in the cultured media of 3T3-L1 preadipocytes were measured using ELISA according to the manufacturer's instructions (R&D Systems, Minneapolis, MN).

Western blot analysis. Two days after confluence, 3T3-L1 preadipocytes were stimulated with 10 ng/ml TNF-α in the absence or presence of 11β-HSD1 inhibitors (50 μM carbenoxolone or 10 μM inhibitor A) for 24 h.

For primary culture experiments, SVF from epididymal fat pads were plated in sixwell plates and cultured overnight in DMEM containing 10% (vol/vol) FBS at 37°C under 10% CO_2. After being rinsed with the medium three times, the cells were incubated with or without TNF-α, carbenoxolone, or inhibitor A for 24 h.

After 2-h serum starvation, cells were treated with TNF-α for 10 min to detect NF-κB and MAPK signals. Cells were washed with ice-cold PBS and harvested in lysis buffer (1% wt/vol SDS, 60 mM Tris · HCl, 1 mM Na_3VO_4, 0.1 mg/ml aprotinin, 1 mM PMSF, and 50 nM okadaic acid at pH 6.8) and boiled at 100°C for 10 min. After centrifugation, supernatants were normalized to the protein concentration via the Bradford method and then equal amounts of protein were subjected to SDS-PAGE and immunoblot analysis.

RNA interference. We tested four different small interfering RNA (siRNA) sequences. Stealth RNAi for mouse 11β-HSD1 (MSS205244, MSS205245, and MSS205246) (Invitrogen), and RNA interference (RNAi) for mouse 11β-HSD1 originally designed by an siRNA Design Support System (TaKaRa Bio, Shiga, Japan; sense: 5′-GAAAUGGCAUAUCAUCUGUTT-3′ and antisense: 3′-TTCUUUACCGUAUAGUAGACA-5′). MSS205245 and MSS205246 did not suppress the 11β-HSD1 mRNA level effectively in preliminary experiments. Therefore, we demonstrated the data of MSS205244 [si(1)] and of the originally designed siRNA [si(2)] in this study. According to the manufacturer's protocol, 3T3-L1 preadipocytes were transfected with 10 nM siRNA in antibiotic-free medium using Lipofectamine RNAiMAX (Invitrogen). We assessed the ransfection efficiency using green fluorescent protein (GFP) detection (pmaxGFP), according to the manufacturer's instructions (Amaxa, Cologne, Germany). Fluorescent microscopic observa-

tion revealed that more than two-thirds of the cells expressed GFP (data not shown).

Expression vector. A mammalian expression vector encoding Hsd11b1 (Hsd11b1/pcDNA3.1) was constructed by inserting cDNA for mouse 11β-HSD1 into pcDNA3.1 (Invitrogen). 3T3-L1 preadipocytes were detached from culture dishes using 0.25% trypsin. Cells (5×10^6) were mixed with 2 μg plasmid in the solution provided with the cell line Nucleofector Kit V (Amaxa). pcDNA3.1/11β-HSD1 or a control vector was introduced into the cells using electroporation with a Nucleofector (Amaxa) instrument according to the manufacturer's instructions.

Statistical analysis. Data are expressed as the means ± SE of triplicate experiments. Data were analyzed using one-way ANOVA, followed by Student's *t*-tests for each pair of multiple comparisons. Differences were considered significant if $P < 0.05$.

RESULTS

Expression of 11β-HSD1 was elevated in the MAF and in SVF isolated from fat depots in ob/ob mice and DIO mice. Genetic (*ob/ob*) and dietary (DIO) obese models were analyzed. Expression of iNOS, MCP-1, and IL-6, all of which are obesity-related proinflammatory mediators (19, 29, 45, 56), was elevated in the MAF and SVF from both *ob/ob* mice and DIO mice compared with lean littermates (Fig. 1, *A* and *B*). Levels of 11β-HSD1 mRNA in the MAF from obese mice were substantially elevated compared with their lean littermates (*ob/ob*: SQ, 5-fold; Mes, 62-fold) (DIO: SQ, 24-fold; Mes, 460-fold; Fig. 1, *A* and *B*). On the other hand, levels of 11β-HSD1 mRNA in SVF from *ob/ob* mice and DIO mice were also elevated compared with their lean littermates (*ob/ob*: SQ, 3-fold; Mes, 3-fold; and DIO: SQ, 8-fold, Mes, 4-fold; Fig. 1, *A* and *B*).

TNF-α, IL-1β, and LPS augmented 11β-HSD1 mRNA expression and reductase activity in 3T3-L1 preadipocytes. When 3T3-L1 preadipocytes were treated with TNF-α (10 ng/ml) for 24 h, mRNA levels of 11β-HSD1 markedly increased (~4-fold; Fig. 2*iv*). Levels of iNOS, MCP-1, and IL-6 mRNA were concomitantly increased (50-, 70-, and 200-fold, respectively; Fig. 2, *i–iii*). IL-1β (1 ng/ml) and LPS (1,000 ng/ml) substantially augmented 11β-HSD1 mRNA expression in 3T3-L1 preadipocytes (10- and 3-fold vs. control, respectively) (Fig. 2*iv*). Reductase activity of 11β-HSD1 was augmented by TNF-α, IL-1β, and LPS compared with the control (2-, 9-, and 6-fold vs. control, respectively; $P < 0.05$; Fig. 2*v*). Based on the results of 11β-HSD1 activity, TNF-α was used at 10 ng/ml in subsequent experiments. On the other hand, 11β-HSD2 mRNA and the corresponding dehydrogenase activity were undetected not only at the baseline condition but with TNF-α, IL-1β, and LPS treatments (data not shown).

Dexamethasone decreased iNOS, MCP-1, and IL-6 mRNA and protein levels in TNF-α-treated 3T3-L1 preadipocytes. The effects of glucocorticoid on proinflammatory gene expression in TNF-α-treated 3T3-L1 preadipocytes were examined over a wide range of concentrations (10^{-10}, 10^{-9}, 10^{-8}, and 10^{-7} M), representing physiological to therapeutical levels in vivo (5). Dexamethasone (10^{-7} M) decreased mRNA levels of iNOS, MCP-1, and IL-6 (iNOS: 85 ± 2%, MCP-1: 40 ± 16%, and IL-6: 97 ± 1% reduction vs. TNF-α-treated cells) and protein levels in the media (MCP-1: 48 ± 5% and IL-6: 83 ± 1% reduction) in TNF-α-treated 3T3-L1 preadipocytes (Suppl. Fig. S1).

Pharmacological inhibition of 11β-HSD1 attenuated iNOS, MCP-1, and IL-6 mRNA and protein levels in TNF-α-treated 3T3-L1 preadipocytes. The effects of pharmacological inhibition of 11β-HSD1 on proinflammatory gene expression were examined in TNFα-treated 3T3-L1 preadipocytes. In previous in vitro studies, carbenoxolone (CBX), a nonselective inhibitor of 11β-HSD1 and 11β-HSD2, was used at concentrations from 5 to 300 μM (16, 17, 26). To date, an 11β-HSD1-specific

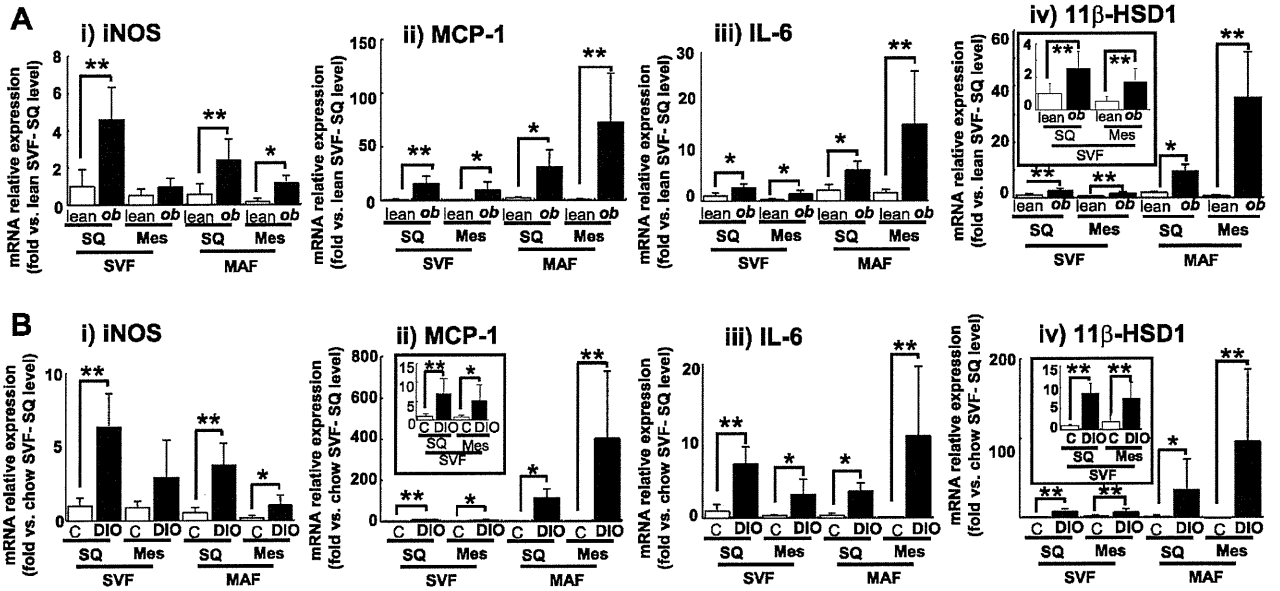

Fig. 1. 11β-Hydroxysteroid dehydrogenase type 1 (11β-HSD1) mRNA expression in stromal vascular fraction cells (SVF) and mature adipocytes fraction (MAF) isolated from obese adipose tissue of *ob/ob* mice and diet-induced obese (DIO) mice. *A*: *ob/ob* and lean littermates [control (C) 9 wk of age; $n = 6$]. *B*: DIO and littermates on a chow diet (17 wk of age; $n = 6$). Levels of inducible nitric oxide synthase (iNOS; *i*), monocyte chemoattractant protein-1 (MCP-1; *ii*), IL-6 (*iii*), and 11β-HSD1 (*iv*) mRNA in SVF and MAF in subcutaneous abdominal fat depots (SQ) and mesenteric fat depots (Mes). *$P < 0.05$, **$P < 0.01$ compared with lean littermates.

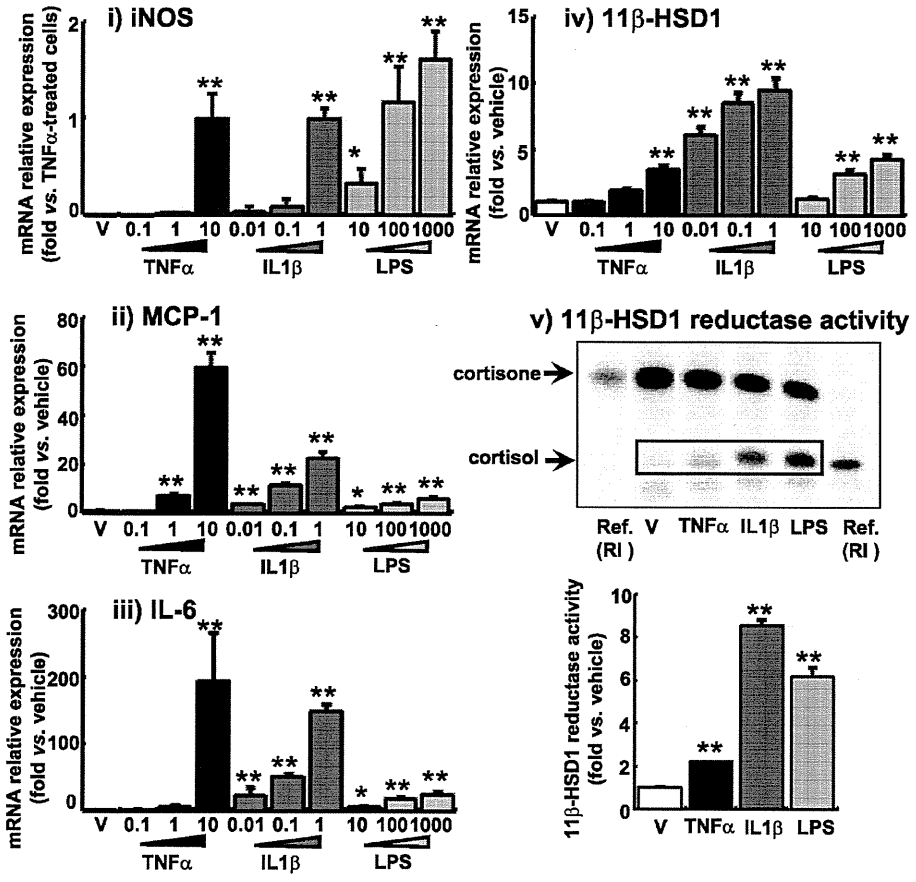

Fig. 2. TNF-α, IL-1β, and LPS augment the expression of proinflammatory mediators and 11β-HSD1 in 3T3-L1 preadipocytes. Cells were treated with TNF-α (0.1, 1, and 10 ng/ml), IL-1β, (0.01, 0.1, and 1 ng/ml) or LPS (10, 100, and 1,000 ng/ml) for 24 h. Levels of iNOS (*i*), MCP-1 (*ii*), IL-6 (*iii*), and 11β-HSD1 (*iv*) mRNA were quantified using real-time PCR. Values were normalized to that of 18S rRNA. *v*: 11β-HSD1 reductase activity (expressed as conversion ability of cortisone to cortisol) was assessed in the medium of 3T3-L1 cells treated with 10 ng/ml TNF-α, 1 ng/ml IL-1β, or 1,000 ng/ml LPS for 24 h. A reference of [^{3}H]cortisone or [^{3}H]cortisol was used as a size marker. A representative autoradiograph of thin-layer chromatography in 11β-HSD reductase activity assay (*top*) and quantification (*bottom*). Intensities of cortisol signals correspond to the enzyme activity of reductase. Ref. (RI), reference samples of [^{3}H]cortisone or [^{3}H]cortisol as size marker. Data are means ± SE of triplicate experiments. $*P < 0.05$, $**P < 0.01$, compared with vehicle (V)-treated group.

inhibitor, inhibitor A, has not been used for in vitro studies; however, another 11β-HSD1-specific inhibitor (compound 544) sharing almost the same structure as inhibitor A was used at a concentration of 5 μM (62). Therefore, in the present study, 10–50 μM CBX and 2.5–10 μM inhibitor A were used.

Before using these inhibitors in intact cells, we validated inhibitory potency of compounds against 11β-HSD1 in the microsome fraction assay. We verified that inhibitor A (10 nM) and CBX (1 μM) inhibited 11β-HSD1 activity as little as 25% vs. control, respectively, and that both of the 11β-HSD inhibitors suppressed 11β-HSD activity in a dose-dependent manner (Suppl. Fig. S2).

In 3T3-L1 preadipocytes, although CBX and inhibitor A did not change the level of 11β-HSD1 reductase activity, both of them suppressed TNF-α-induced reductase activity of 11β-HSD1 in a dose-dependent manner (Fig. 3*A*). CBX (50 μM) and inhibitor A (10 μM) markedly attenuated 11β-HSD1 activity (78 and 60% reduction vs. TNF-α-treated cells, respectively; Fig. 3*A*).

Without TNF-α-treatment, CBX and inhibitor A did not affect mRNA or protein levels of iNOS, MCP-1, and IL-6. On the other hand, in TNF-α-treated cells, these inhibitors reduced the mRNA and protein levels of proinflammatory genes. CBX decreased iNOS, MCP-1, and IL-6 mRNA levels (50 μM; iNOS: 83 ± 5%, MCP-1: 27 ± 4%, and IL-6: 47 ± 10% reduction vs. TNF-α-treated cells without compounds) and protein levels in the media (MCP-1: 17 ± 1% and IL-6: 34 ± 6% reduction) in TNF-α-treated 3T3-L1 preadipocytes (Fig. 3*B*). Similarly, inhibitor A reduced iNOS, MCP-1, and IL-6 mRNA (10 μM; iNOS: 47 ± 13%, MCP-1: 32 ± 12%, and IL-6: 33 ± 9% reduction) and protein levels in the media (MCP-1: 47 ± 3% and IL-6: 14 ± 3% reduction) (Fig. 3*C*).

Effect of 11β-HSD1 knockdown on proinflammatory properties in 3T3-L1 preadipocytes. To explore the potential role of 11β-HSD1 in cytokine release from activated preadipocytes, 11β-HSD1 was knocked down using siRNA. We tested four different siRNA sequences as described in MATERIALS AND METHODS; however, two of them did not suppress 11β-HSD1 mRNA level significantly in the preliminary experiments. Thus we demonstrated the data on si(1) and si(2).

When 3T3-L1 preadipocytes were transfected with 11β-HSD1 siRNA, TNF-α-induced expression of 11β-HSD1 was markedly attenuated [si(1): 60 ± 9% and si(2): 88 ± 7% reduction vs. negative control siRNA; Fig. 4*A*, *i*]. 11β-HSD1 reductase activity was also decreased by 11β-HSD1 siRNA [si(1): 81 ± 9% and si(2): 84 ± 3% reduction vs. negative control siRNA; Fig. 4*A*, *ii*]. 11β-HSD2 mRNA levels and the corresponding dehydrogenase activity were under detectable with or without siRNA treatments in 3T3-L1 preadipocytes (data not sown). Negative control RNAi did not influence the expression of 11β-HSD1. Knockdown of 11β-HSD1 in TNF-α-treated 3T3-L1 preadipocytes effectively reduced iNOS, MCP-1, and IL-6 mRNA levels [si(1): IL-6: 32 ± 7% reduction; and si(2): iNOS: 37 ± 8%, MCP-1: 22 ± 5%, and IL-6: 59 ± 3% reduction] and protein levels in the media [si(1):

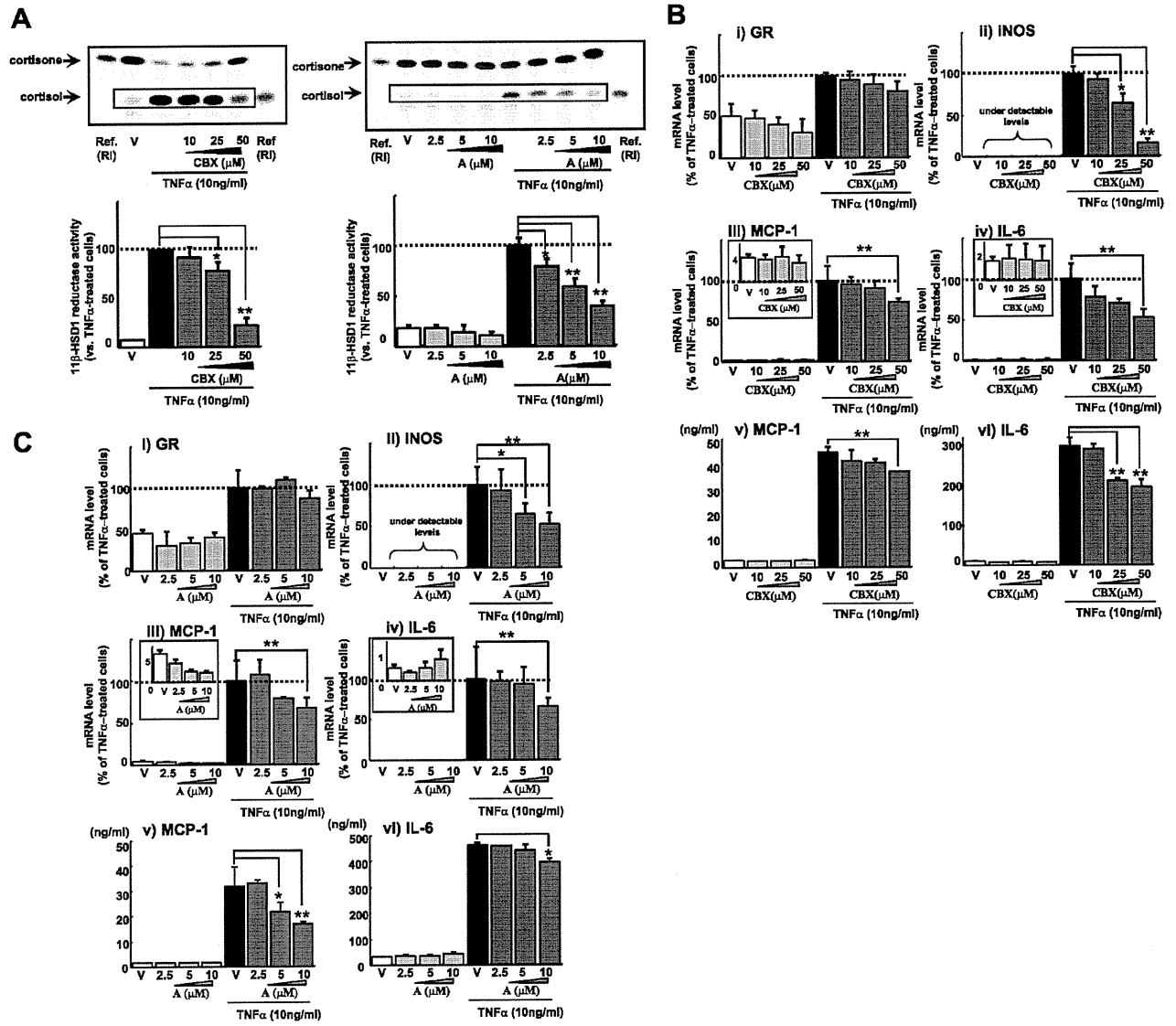

Fig. 3. Effects of pharmacological inhibition of 11β-HSD1 on glucocorticoid receptor (GR), MCP-1, IL-6, and iNOS expression in and secretion from TNF-α-treated 3T3-L1 preadipocytes. *A*: 11β-HSD1 activity assay for validation of 11β-HSD1 inhibitors. 3T3-L1 preadipocytes were incubated for 24 h in serum-free DMEM, adding 250 nM of cortisone with tritium-labeled cortisone. A representative autoradiograph of TLC for the 11β-HSD1 activity assay (*top*) and quantification of 11β-HSD1 activities (*bottom*). Intensities of cortisol signals correspond to the reductase activity. The *y*-axis shows percent 11β-HSD1 reductase activity compared with TNF-α (10 mg/ml)-treated cells. carbenoxolone (CBX; 10–50 μM) and inhibitor A (A; 2.5–10 μM) substantially reduced 11β-HSD1 activity in 3T3-L1 preadipocytes. CBX (*B*; 10–50 μM) and inhibitor A (*C*; 2.5–10 μM) 3T3-L1 preadipocytes were treated with TNF-α (10 ng/ml) or cotreated with CBX and inhibitor A for 24 h. GR (*i*), iNOS (*ii*), MCP-1 (*iii*), and IL-6 (*iv*) mRNA levels were determined using real-time PCR. Values were normalized to that of 18S rRNA and expressed relative to TNF-α-treated cells. Concentrations of MCP-1 (*v*) and IL-6 (*vi*) in the medium were measured with ELISA. Data are means ± SE of triplicate experiments. $*P < 0.05$, $** P < 0.01$, compared with TNF-α-treated cells.

MCP-1: 13 ± 1% and IL-6: 17 ± 1% reduction; and si(2): MCP1: 19 ± 7% and IL-6: 30 ± 1% reduction; Fig. 4*B*].

Overexpression of 11β-HSD1 augmented iNOS, MCP-1, and IL-6 in TNF-α-treated 3T3-L1 preadipocytes. We examined whether overexpression of 11β-HSD1 is relevant to the augmentation of proinflammatory molecules in activated preadipocytes. The extent of 11β-HSD1 overexpression in 3T3-L1 preadipocytes was assessed by 11β-HSD1 mRNA levels and reductase activity (Fig. 5*A*). As expected, 11β-HSD1 mRNA level was increased by treatment of the 11β-HSD1 vector (~20-fold) or 10 ng/ml TNF-α (~300-fold) compared with the vehicle. TNF-α-induced expression of 11β-HSD1 was further augmented by the introduction of the 11β-HSD1 vector (1.6-fold vs. empty vector). Reductase activity of 11β-HSD1 was also increased by the introduction of the vector (2-fold) or 10 ng/ml TNF-α (10-fold). Notably, TNF-α-induced enzyme activity was further augmented by the vector (1.3-fold vs. empty vector).

Expression of iNOS, MCP-1, and IL-6 did not differ between the 11β-HSD1 vector and the empty vector. On the other hand, TNF-α-induced expression of iNOS, MCP-1, and IL-6 was augmented in 11β-HSD1 transfectants (MCP-1: 172 ±

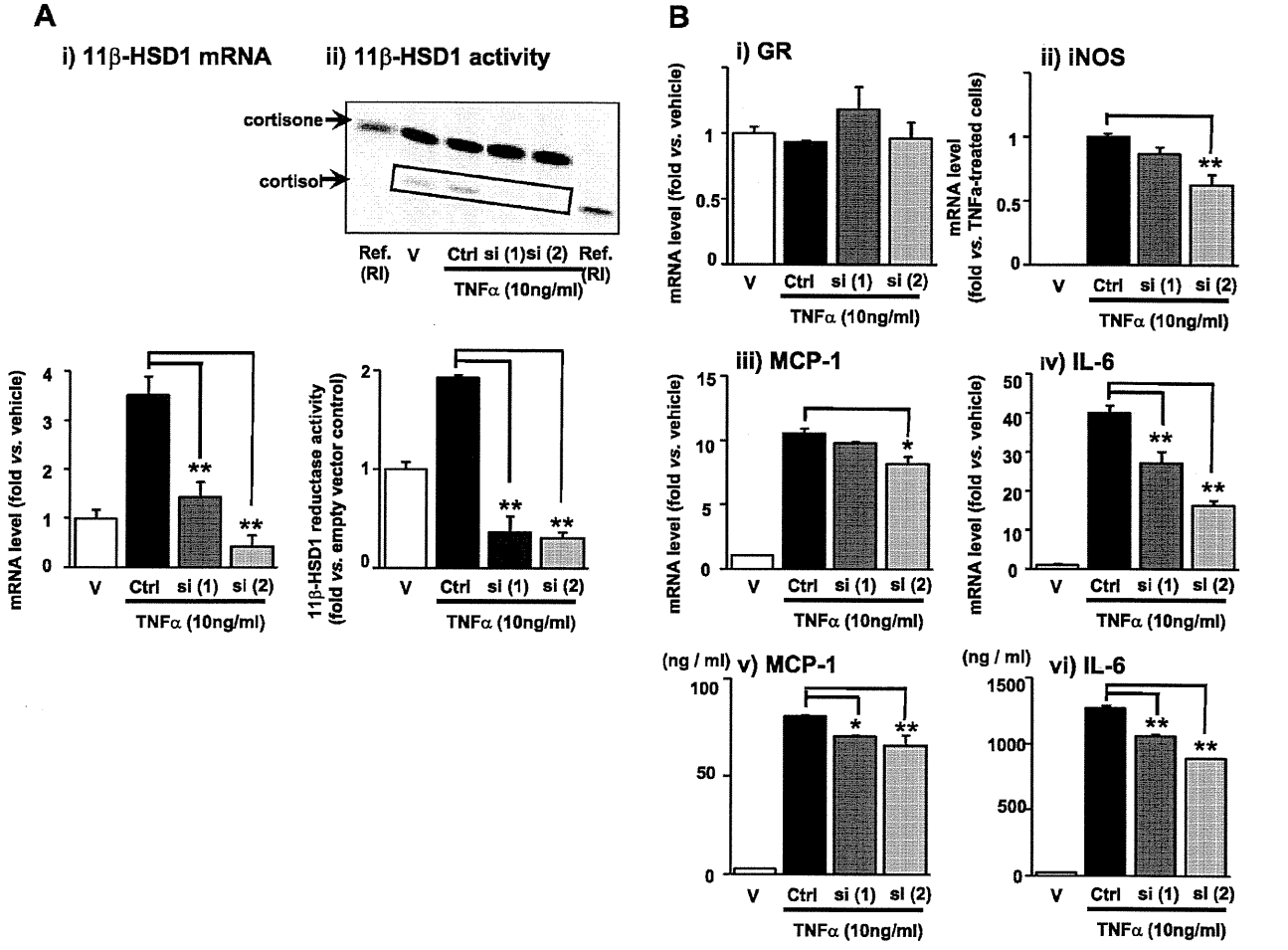

Fig. 4. Effects of 11β-IISD1 knockdown on TNF-α-induced expression of 11β-IISD1 in 3T3-L1 preadipocytes. Cells were transfected with either RNA interference for mouse 11β-HSD1 or a negative control (Ctrl). After 12 h incubation, cells were treated with 10 ng/ml TNF-α for 24 h. *A*: efficiency of 11β-HSD1 knockdown by small-interfering RNA. 11β-HSD1 mRNA (*i*) and reductase activity (*ii*). *B*: effects of knockdown of 11β-HSD1 on MCP-1, IL-6, and iNOS expression in and secretion from TNFα-treated 3T3-L1 preadipocytes. 11β-HSD1 (*i*), GR (*ii*), iNOS (*iii*), MCP-1 (*iv*), and IL-6 mRNA (*v*) levels were determined using real-time PCR. Values were normalized to that of 18S rRNA and expressed as a relative level vs. vehicle control (V). Concentrations of MCP-1 (*vi*) and IL-6 (*vii*) in the medium were measured with ELISA. Data are means ± SE of triplicate experiments. $*P < 0.05$, $**P < 0.01$, compared with TNF-α-treated cells. siRNA for mouse 11β-HSD1: si(1): MSS205244 (Invitrogen) and si(2): sense: 5′-GAAAUGGCAUAUCAUCUGUTT-3′ and antisense: 3′-TTCUUUACCGUAUAGUAGACA-5′ (Takara).

88%, IL-6: 194 ± 64%, and iNOS: 187 ± 47% vs. the empty vector; Fig. 5*B*, *ii-iv*). Similarly, protein levels of MCP-1 and IL-6 in the media were increased in transfectants (MCP-1: 206 ± 32% and IL-6: 156 ± 17% vs. the empty vector; Fig. 5*B*, *v* and *vi*).

Pharmacological inhibition of 11β-HSD1 attenuated TNF-α-induced NF-κB and MAPK signaling in 3T3-L1 preadipocytes. We examined the possible involvement of 11β-HSD1 in proinflammatory signaling pathways. 3T3-L1 preadipocytes were incubated with TNF-α (10 ng/ml), with or without CBX (50 μM) and inhibitor A (10 μM) for 24 h. After a 2-h serum starvation, the cells were incubated with TNF-α (10 ng/ml), with or without CBX (50 μM) and inhibitor A (10 μM) for 10 min. TNF-α-induced p-65 phosphorylation was markedly attenuated by CBX (30 ± 12% decrease vs. TNF-α-treated cells) and inhibitor A (51 ± 11% decrease vs. TNF-α-treated cells; Fig. 6*A*). Regarding MAPK signaling, augmented phosphorylation of p-38, JNK, and ERK with the TNF-α treatment was substantially attenuated by CBX (p-38: 26 ± 8% decrease and JNK: 48 ± 3% decrease vs. TNF-α-treated cells) and inhibitor A (p-38: 51 ± 9% decrease, JNK: 72 ± 5% decrease, and ERK: 36 ± 11% decrease vs. TNF-α-treated cells; Fig. 6*B*).

Pharmacological inhibition of 11β-HSD1 attenuated iNOS, MCP-1, and IL-6 mRNA levels in SVF cells from ob/ob mice. We examined the effects of pharmacological inhibition of 11β-HSD1 on proinflammatory gene expression in primary cultured SVF cells isolated from epididymal fat depots in obese *ob/ob* mice or lean control mice.

CBX (50 μM) and inhibitor A (10 μM) did not change the expression level of 11β-HSD1 (Fig. 7*i*). CBX decreased mRNA level of iNOS, MCP-1, and IL-6 in both the basal state (iNOS: 69 ± 4%, MCP1: 42 ± 7%, and IL-6: 56 ± 14% reduction vs. vehicle control) and TNFα-stimulated state (iNOS: 58 ± 11%, MCP-1: 63 ± 5%, and IL-6: 53 ± 8% reduction vs. TNFα-treated cells without compounds) in SVF cells from *ob/ob* mice.

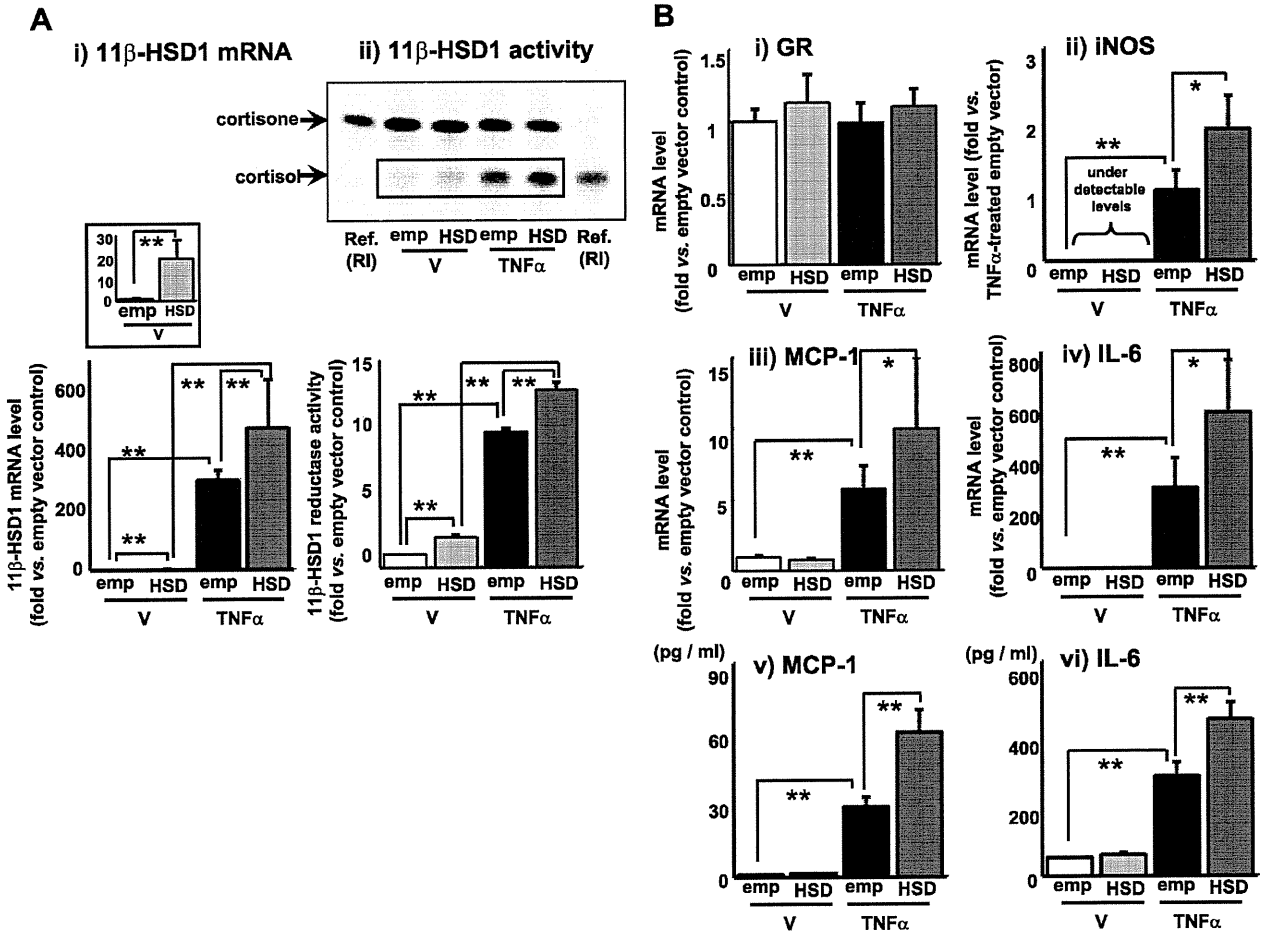

Fig. 5. Effects of overexpression of 11β-HSD1 on MCP-1, IL-6, and iNOS expression in and secretion from TNF-α-treated 3T3-L1 preadipocytes. *A*: efficiency of electroporation-mediated gene transfer. 3T3-L1 preadipocytes were transfected with the expression vector for 11β-HSD1 or a corresponding empty vector using electroporation. After 48 h, cells were treated with or without 10 ng/ml TNF-α for 24 h. Cells were assayed for 11β-HSD1 mRNA (*i*) and reductase activity (*ii*). *B*: effects of overexpression of 11β-HSD1 on MCP-1, IL-6, and iNOS expression in and secretion from TNF-α-treated 3T3-L1 preadipocytes. 3T3-L1 preadipocytes were transfected as above, and 48 h after the infection, cells were treated with or without 10 ng/ml TNF-α for 24 h. Levels of mRNA for GR (*i*), iNOS (*ii*), MCP-1 (*iii*), and IL-6 (*iv*) were determined using real-time PCR. Values were normalized to those of 18S rRNA and expressed as a relative level vs. the vehicle control (V). Concentrations of MCP-1 (*v*) and IL-6 (*vi*) in the medium were measured with ELISA. Data are means ± SE of triplicate experiments. $*P < 0.05$, $**P < 0.01$.

Without TNF-α-treatment, CBX did not change mRNA levels of iNOS, MCP-1 and IL-6 in SVF cells from lean control mice. However, CBX reduced the mRNA levels of iNOS, MCP-1, and IL-6 (iNOS: 64 ± 18%, MCP-1: 67 ± 14%, and IL-6: 58 ± 12% reduction vs. TNF-α-treated cells without compounds) in TNF-α-treated SVF cells from lean control mice (Fig. 7).

Pharmacological inhibition of 11β-HSD1 attenuated NF-κB and MAPK signaling in SVF cells from ob/ob mice. SVF cells from *ob/ob* or lean control mice were incubated with TNF-α (10 ng/ml), with or without CBX (50 μM) and inhibitor A (10 μM) for 24 h. After a 2-h serum starvation, the cells were incubated with TNF-α (10 ng/ml), with or without CBX (50 μM) and inhibitor A (10 μM) for 10 min. Activation of NF-κB (p65) and MAPK (p38, JNK, and ERK) signaling did occur in SVF cells from *ob/ob* mice compared with lean control (Suppl. Fig. S3). In *ob/ob* mice, phosphorylation of these signaling without TNF-α treatment was attenuated by CBX and inhibitor A. TNF-α-induced p-65, p38, JNK, and ERK phosphorylation was also attenuated by CBX and inhibitor A in SVF cells from both *ob/ob* and lean control mice (Suppl. Fig. S3).

DISCUSSION

Here we provide novel evidence that inflammatory stimuli-induced 11β-HSD1 in activated preadipocytes intensifies NF-κB and MAPK signaling pathways and the resultant augmentation of proinflammatory molecules. Not limited to 3T3-L1 preadipocytes, we also demonstrated the notion was reproducible in the primary SVF cells from obese mice. Previous works focused on the metabolically beneficial impact of 11β-HSD1 deficiency on adipose tissue distribution, fuel homeostasis, and insulin sensitivity. On the other hand, clearly distinct from previous works, our present study is the first to highlight an unexpected, proinflammatory role of reamplified glucocorticoids within activated preadipocytes in obese adipose tissue.

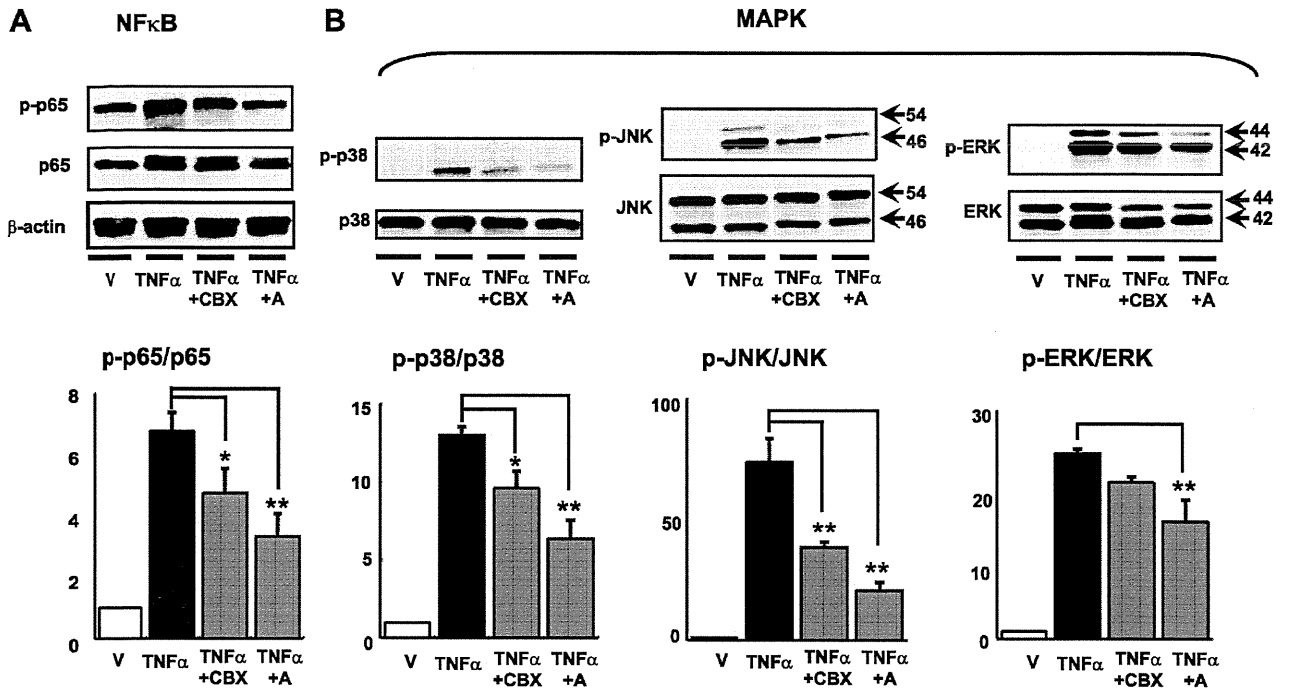

Fig. 6. Effects of inhibition of 11β-HSD1 on TNF-α-induced NFκB and MAPK signaling. NFκB (*A*) and MAPK (*B*) signaling pathways. 3T3-L1 preadipocytes were treated with 10 ng/ml TNF-α for 24 h in the presence or absence of 11β-HSD1 inhibitors (CBX or inhibitor A). After 2-h serum starvation, cells were treated with TNF-α in the presence or absence of 11β-HSD1 inhibitors for 10 min to assess the activation of NFκB and MAPK signaling pathways. Western blot analyses were performed using antibodies against β-actin and NFκB-p65 (*A*), phospho-p65 (*B*), p38-MAPK (*B, left*), phospho-p38 (*B, center*) JNK, phospho-JNK (*B, right*) ERK 1/2, and phospho-ERK1/2. A representative Western blot (*top*) and quantification of p65, p38, JNK, and ERK phosphorylation (*bottom*). Data are means ± SE of triplicate experiments. $^*P < 0.05$, $^{**}P < 0.01$ compared with TNF-α-treated cells.

Suppression and overexpression experiments with 11β-HSD1 in activated preadipocytes demonstrate that TNF-α-induced 11β-HSD1 further augments the expression of proinflammatory genes including iNOS, MCP-1, and IL-6. Elevation of iNOS, MCP-1, and IL-6 in adipose tissue is commonly observed in obese subjects, linking to dysfunction of adipose tissue (19, 29, 45, 56). For example, iNOS-deficient mice are protected against obesity-induced insulin resistance and glucose intolerance (45). Moreover, transgenic mice overexpressing MCP-1 in adipose tissue exemplify insulin resistance and exaggerated infiltration of macrophages into adipose tissue (29). Previous studies (20, 36) showed that adipose tissue is a primary production site for IL-6 in humans. In fact, circulating IL-6 levels are shown to elevate in patients with insulin-resistance (19, 56), impaired glucose tolerance (40), and type 2 diabetes (47). Taken together, the present study provides novel evidence for proinflammatory role of 11β-HSD1 in activated preadipocytes.

To optimize experimental condition, the present study was designed to eliminate possible toxic effects and nonspecific effects of 11β-HSD1 inhibitors. Because 11β-HSD2 mRNA and corresponding dehydrogenase enzyme activity (8, 27) were undetected in 3T3-L1 preadipocytes even after the treatment with TNF-α (unpublished observations), CBX virtually serves as a specific inhibitor against 11β-HSD1 in the present study. To further verify the effect of 11β-HSD1 inhibition on activated preadipocytes, we confirmed that an 11β-HSD1-specific inhibitor A exerted similar effects to CBX (Fig. 3). Of note, the expression level of the glucocorticoid receptor did not vary by the treatment with 11β-HSD1 inhibitors (unpublished observations). The notion that TNF-α-induced 11β-HSD1 would reinforce the expression of proinflammatory genes was endorsed by the results of RNAi experiments (Fig. 4) and overexpression experiments (Fig. 5). It should be emphasized that forced overexpression of 11β-HSD1 per se did not influence the expression level of proinflammatory genes in nonactivated preadipocytes (Fig. 5*B*). These findings led us to speculate that 11β-HSD1-mediated active glucoorticoids within cells reinforce inflammation under proinflammatory conditions commonly seen in obese adipose tissue.

The present study demonstrated that 11β-HSD1 was highly expressed in SVF cells from obese adipose tissue (Fig. 1). Although mature adipocytes abundantly express 11β-HSD1 (44, 61), a considerable amount of 11β-HSD1 expression was detected in SVF from adipose tissue (Fig. 1). Potential link between preadipocyte function and pathophysiology of obese adipose tissue has recently attracted research interest (53, 57). A recent study (14) using 11β-HSD1 knockout mice provided evidence that 11β-HSD1 in preadipocytes may affect fat distribution under overnutrition. In 3T3-L1 cells, the expression level of 11β-HSD1 is lower in preadipocytes but is dramatically increased during the course of differentiation into mature adipocytes (51). In fact, active glucocorticoids generated intracellularly by 11β-HSD1 are critical for normal adipose differentiation (33). On the other hand, TNF-α augments 11β-HSD1 expression in preadipocytes (Fig. 2). Of note, in proinflammatory milieu, TNF-α inhibits adipocyte differentiation by decreasing PPARγ expression (43, 46, 64). Depending on the

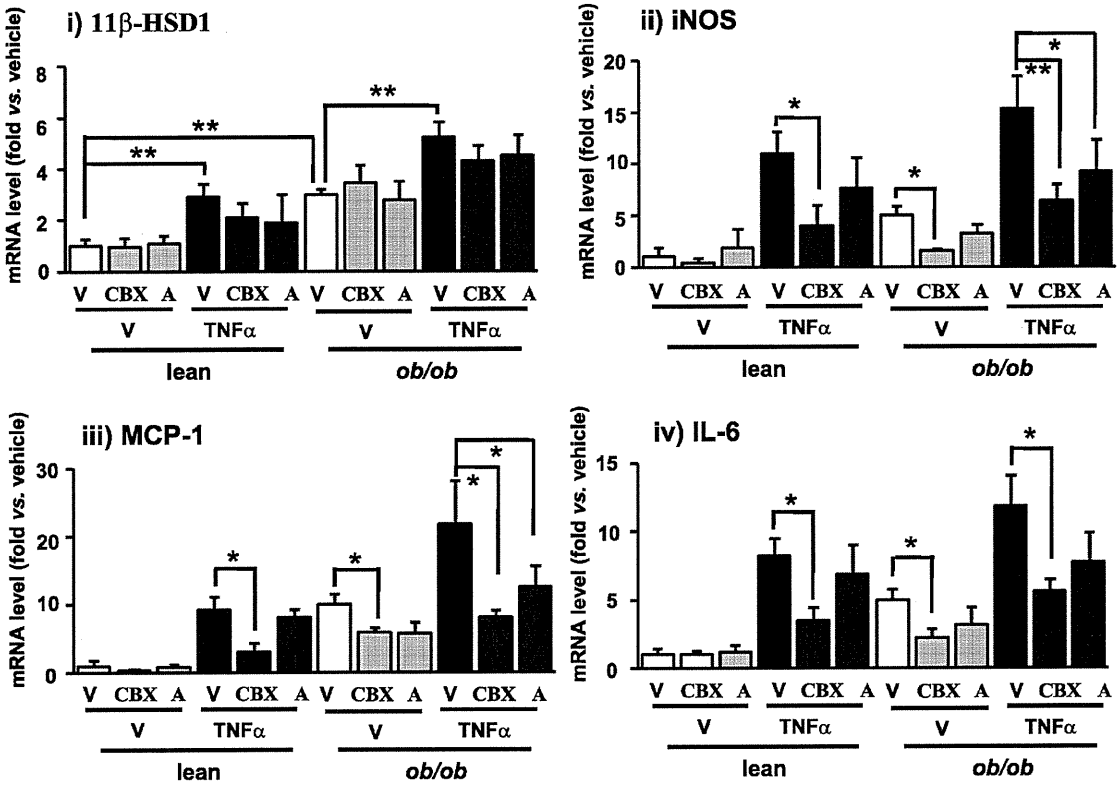

Fig. 7. Effects of pharmacological inhibition of 11β-HSD1 on iNOS, MCP-1, and IL-6 mRNA levels in SVF cells from *ob/ob* mice. SVF cells from *ob/ob* mice and lean control mice were treated with CBX (50 μM) or inhibitor A (10 μM), with or without TNF-α (10 ng/ml) for 24 h. 11β-HSD1 (*i*), iNOS (*ii*), MCP-1 (*iii*), and IL-6 mRNA (*iv*) levels were determined using real-time PCR. Values were normalized to that of 18S rRNA and expressed relative to lean control. Data are means ± SE of triplicate experiments. $^{*}P < 0.05$, $^{**}P < 0.01$.

hormonal milieu, it is therefore conceivable that 11β-HSD1 plays a role in both adipogenesis and inflammatory response in preadipoytes.

We assessed the expression of Pref-1 (a representative molecular marker for preadipocytes; Ref. 7) as well as aP2, PPARγ2, and GLUT4 (a set of representative markers for differentiated adipocytes; Refs. 32 and 59) in preadipocytes overexpressing 11β-HSD1. Consequently, forced augmentation of 11β-HSD1 did not affect the expression level of these genes (Suppl. Fig. S4), supporting that a line of our observation was not a facet of mature adipocytes but of preadipocytes.

Previous studies demonstrated that chronic inflammation is closely associated with insulin resistance in insulin-sensitive organs (24, 64). Glucocorticoids are widely used as anti-inflammatory agents in a clinical setting (49). On the other hand, this hormone simultaneously causes insulin resistance (4, 50). Regarding this apparent paradox, recent studies (34, 55) suggest that reactivated glucocorticoids within cells have the potential to enhance inflammatory or immune responses in a variety of cells. In the present study, replenished dexamethasone in the culture media at pharmacological doses did decrease the synthesis and secretion of proinflammatory molecules in preadipocytes in a dose-dependent manner (Fig. 3). On the other hand, in activated preadipocytes, 11β-HSD1 intensifies TNF-α-induced activation of NF-κB and the MAPK signaling cascade (Fig. 6). In this context, it is possible that intracellular activation of glucocorticoids within physiological range would likely cause proinflammatory responses in certain cell types. It should be noted that preadipocytes possess very few insulin receptors (51). Instead, preadipocytes express a large number of IGF-1 receptors (18). Insulin can bind to the IGF-1 receptor only at supraphysiological concentrations. However, it is likely that increased release of inflammatory cytokines from activated preadipocytes may aggravate insulin receptor signaling in adjacent mature adipocytes in obese adipose tissue. This notion is supported by a line of mouse experiments showing that pharmacological inhibition of 11β-HSD1 ameliorated diabetes, dyslipidemia, and even arteriosclerosis (1, 23).

PPARγ agonists potently suppress the activity of 11β-HSD1 exclusively in adipose tissue (6). The present finding that amplified glucocorticoids within activated preadipocytes may enhance inflammatory responses does not contradict the notion that PPARγ agonists exert potent anti-inflammatory effects in a variety of cell types (37).

Recent studies showed that phosphoinositide 3-kinase (PI3K)-Akt pathways, IL-1 receptor-associated kinase-M (IRAK-M), and suppressors of cytokine signaling-1 (SOCS-1) are negative regulators of NF-κB and MAPK signaling (21). Under inflammatory stimuli, a physiological dose of glucocorticoids positively regulates the expression of SHIP1, a phosphatase that negatively regulates PI3K signaling, resulting in the activation of NF-κB and MAPK in activated macrophages (67). Considering the close biological similarities between activated preadipocytes and activated macrophages (11, 13), we explored whether PI3K-Akt pathways, SHIP1, or other phosphatases could be

involved in the 11β-HSD1-induced NF-κB and MAPK activation. Western blot analyses indicated that phosphorylation of Akt or protein levels of SHIP1, PP2A, or MKP-1 did not change significantly with inhibition or overexpression of 11β-HSD1 (Suppl. Fig. S5). Further studies are warranted to unravel the entire mechanism.

In summary, the present study provides novel evidence that inflammatory stimuli-induced 11β-HSD1 reinforces NF-κB and MAPK signaling pathways and results in further induction of proinflammatory molecules in activated preadipocytes. Our findings highlight an unexpected, inflammatory role of reactivated glucocorticoids within preadipocytes in obese adipose tissue.

ACKNOWLEDGMENTS

We thank A. Ryu, S. Maki, M. Nagamoto, T. Fukui, Y. Kobayashi, S. Yamauchi, and K. Takahashi for assistance.

GRANTS

This work was supported in part by a Grant-in-Aid for Scientific Research (B2:19390248), the Takeda Medical Research Foundation, and the Lilly Research Foundation.

DISCLOSURES

No conflicts of interest are declared by the author(s).

REFERENCES

1. **Alberts P, Nilsson C, Selen G, Engblom LO, Edling NH, Norling S, Klingstrom G, Larsson C, Forsgren M, Ashkzari M, Nilsson CE, Fiedler M, Bergqvist E, Ohman B, Bjorkstrand E, Abrahmsen LB.** Selective inhibition of 11 beta-hydroxysteroid dehydrogenase type 1 improves hepatic insulin sensitivity in hyperglycemic mice strains. *Endocrinology* 144: 4755–4762, 2003.
2. **Andrew R, Phillips DI, Walker BR.** Obesity and gender influence cortisol secretion and metabolism in man. *J Clin Endocrinol Metab* 83: 1806–1809. 1998.
3. **Andrews RC, Rooyackers O, Walker BR.** Effects of the 11 beta-hydroxysteroid dehydrogenase inhibitor carbenoxolone on insulin sensitivity in men with type 2 diabetes. *J Clin Endocrinol Metab* 88: 285–291, 2003.
4. **Asensio C, Muzzin P, Rohner-Jeanrenaud F.** Role of glucocorticoids in the physiopathology of excessive fat deposition and insulin resistance. *Int J Obes Relat Metab Disord* 28 *Suppl* 4: S45–52, 2004.
5. **Balachandran A, Guan H, Sellan M, van Uum S, Yang K.** Insulin and dexamethasone dynamically regulate adipocyte 11beta-hydroxysteroid dehydrogenase type 1. *Endocrinology* 149: 4069–4079, 2008.
6. **Berger J, Tanen M, Elbrecht A, Hermanowski-Vosatka A, Moller DE, Wright SD, Thieringer R.** Peroxisome proliferator-activated receptor-gamma ligands inhibit adipocyte 11beta-hydroxysteroid dehydrogenase type 1 expression and activity. *J Biol Chem* 276: 12629–12635, 2001.
7. **Boney CM, Fiedorek FT Jr, Paul SR, Gruppuso PA.** Regulation of preadipocyte factor-1 gene expression during 3T3-L1 cell differentiation. *Endocrinology* 137: 2923–2928, 1996
8. **Bujalska IJ, Kumar S, Stewart PM.** Does central obesity reflect "Cushing's disease of the omentum"? *Lancet* 349: 1210–1213, 1997.
9. **Cancello R, Henegar C, Viguerie N, Taleb S, Poitou C, Rouault C, Coupaye M, Pelloux V, Hugol D, Bouillot JL, Bouloumie A, Barbatelli G, Cinti S, Svensson PA, Barsh GS, Zucker JD, Basdevant A, Langin D, Clement K.** Reduction of macrophage infiltration and chemoattractant gene expression changes in white adipose tissue of morbidly obese subjects after surgery-induced weight loss. *Diabetes* 54: 2277–2286, 2005.
10. **Chapman KE, Coutinho AE, Gray M, Gilmour JS, Savill JS, Seckl JR.** The role and regulation of 11beta-hydroxysteroid dehydrogenase type 1 in the inflammatory response. *Mol Cell Endocrinol* 301: 123–131, 2009.
11. **Charriere G, Cousin B, Arnaud E, Andre M, Bacou F, Penicaud L, Casteilla L.** Preadipocyte conversion to macrophage. Evidence of plasticity. *J Biol Chem* 278: 9850–9855, 2003.
12. **Chung S, Lapoint K, Martinez K, Kennedy A, Boysen Sandberg M, McIntosh MK.** Preadipocytes mediate lipopolysaccharide-induced inflammation and insulin resistance in primary cultures of newly differentiated human adipocytes. *Endocrinology* 147: 5340–5351, 2006.
13. **Cousin B, Munoz O, Andre M, Fontanilles AM, Dani C, Cousin JL, Laharrague P, Casteilla L, Penicaud L.** A role for preadipocytes as macrophage-like cells. *FASEB J* 13: 305–312, 1999.
14. **De Sousa Peixoto RA, Turban S, Battle JH, Chapman KE, Seckl JR, Morton NM.** Preadipocyte 11beta-hydroxysteroid dehydrogenase type 1 is a keto-reductase and contributes to diet-induced visceral obesity in vivo. *Endocrinology* 149: 1861–1868, 2008.
16. **Dembinska-Kiec A, Pallapies D, Simmet T, Peskar BM, Peskar BA.** Effect of carbenoxolone on the biological activity of nitric oxide: relation to gastroprotection. *Br J Pharmacol* 104: 811–816, 1991.
17. **Elsen FP, Shields EJ, Roe MT, Vandam RJ, Kelty JD.** Carbenoxolone induced depression of rhythmogenesis in the pre-Botzinger complex. *BMC Neurosci* 9: 46, 2008.
18. **Entingh-Pearsall A, Kahn, CR.** Differential roles of the insulin and insulin-like growth factor-i (igf-i) receptors in response to insulin and IGF-I. *J Biol Chem* 279: 38016–38024, 2004.
19. **Fernandez-Real JM, Vayreda M, Richart C, Gutierrez C, Broch M, Vendrell J, Ricart W.** Circulating interleukin 6 levels, blood pressure, and insulin sensitivity in apparently healthy men and women. *J Clin Endocrinol Metab* 86: 1154–1159, 2001.
20. **Fried SK, Bunkin DA, Greenberg AS.** Omental and subcutaneous adipose tissues of obese subjects release interleukin-6: depot difference and regulation by glucocorticoid. *J Clin Endocrinol Metab* 83: 847–850, 1998.
21. **Fukao T, Koyasu S.** PI3K and negative regulation of TLR signaling. *Trends Immunol* 24: 358–363, 2003.
22. **Hauner H.** Secretory factors from human adipose tissue and their functional role. *Proc Nutr Soc* 64: 163–169, 2005.
23. **Hermanowski-Vosatka A, Balkovec JM, Cheng K, Chen HY, Hernandez M, Koo GC, Le Grand CB, Li Z, Metzger JM, Mundt SS, Noonan H, Nunes CN, Olson SH, Pikounis B, Ren N, Robertson N, Schaeffer JM, Shah K, Springer MS, Strack AM, Strowski M, Wu K, Wu T, Xiao J, Zhang BB, Wright SD, Thieringer R.** 11beta-HSD1 inhibition ameliorates metabolic syndrome and prevents progression of atherosclerosis in mice. *J Exp Med* 202: 517–527, 2005.
24. **Hotamisligil GS.** Inflammation and metabolic disorders. *Nature* 444: 860–867, 2006.
25. **Hult M, Shafqat N, Elleby B, Mitschke D, Svensson S, Forsgren M, Barf T, Vallgarda J, Abrahmsen L, Oppermann U.** Active site variability of type 1 11beta-hydroxysteroid dehydrogenase revealed by selective inhibitors and cross-species comparisons. *Mol Cell Endocrinol* 248: 26–33, 2006.
26. **Ishii T, Masuzaki H, Tanaka T, Arai N, Yasue S, Kobayashi N, Tomita T, Noguchi M, Fujikura J, Ebihara K, Hosoda K, Nakao K.** Augmentation of 11beta-hydroxysteroid dehydrogenase type 1 in LPS-activated J774.1 macrophages–role of 11beta-HSD1 in pro-inflammatory properties in macrophages. *FEBS Lett* 581: 349–354, 2007.
27. **Jamieson PM, Chapman KE, Edwards CR, Seckl JR.** 11 beta-hydroxysteroid dehydrogenase is an exclusive 11 beta- reductase in primary cultures of rat hepatocytes: effect of physicochemical and hormonal manipulations. *Endocrinology* 136: 4754–4761, 1995.
28. **Julien P, Despres JP, Angel A.** Scanning electron microscopy of very small fat cells and mature fat cells in human obesity. *J Lipid Res* 30: 293–299, 1989.
29. **Kanda H, Tateya S, Tamori Y, Kotani K, Hiasa K, Kitazawa R, Kitazawa S, Miyachi H, Maeda S, Egashira K, Kasuga M.** MCP-1 contributes to macrophage infiltration into adipose tissue, insulin resistance, and hepatic steatosis in obesity. *J Clin Invest* 116: 1494–1505, 2006.
30. **Kershaw EE, Morton NM, Dhillon H, Ramage L, Seckl JR, Flier JS.** Adipocyte-specific glucocorticoid inactivation protects against diet-induced obesity. *Diabetes* 54: 1023–1031, 2005.
31. **Kotelevtsev Y, Holmes MC, Burchell A, Houston PM, Schmoll D, Jamieson P, Best R, Brown R, Edwards CR, Seckl JR, Mullins JJ.** 11beta-hydroxysteroid dehydrogenase type 1 knockout mice show attenuated glucocorticoid-inducible responses and resist hyperglycemia on obesity or stress. *Proc Natl Acad Sci USA* 94: 14924–14929, 1997.
32. **Lane MD, Tang QQ, Jiang MS.** Role of the CCAAT enhancer binding proteins (C/EBPs) in adipocyte differentiation. *Biochem Biophys Res Commun* 266: 677–683, 1999.

33. **Liu Y, Sun Y, Zhu T, Xie Y, Yu J, Sun WL, Ding GX, Hu G.** 11β HSD1 promotes differentiation of 3T3-L1 preadipocyte. *Acta Pharmacol Sin* 28: 1198–204, 2007.
34. **McEwen BS, Biron CA, Brunson KW, Bulloch K, Chambers WH, Dhabhar FS, Goldfarb RH, Kitson RP, Miller AH, Spencer RL, Weiss JM.** The role of adrenocorticoids as modulators of immune function in health and disease: neural, endocrine and immune interactions. *Brain Res Brain Res Rev* 23: 79–133, 1997.
35. **McLaughlin T, Sherman A, Tsao P, Gonzalez O, Yee G, Lamendola C, Reaven GM, Cushman SW.** Enhanced proportion of small adipose cells in insulin-resistant vs insulin-sensitive obese individuals implicates impaired adipogenesis. *Diabetologia* 50: 1707–1715, 2007.
36. **Mohamed-Ali V, Goodrick S, Rawesh A, Katz DR, Miles JM, Yudkin JS, Klein S, Coppack SW.** Subcutaneous adipose tissue releases interleukin-6, but not tumor necrosis factor-alpha, in vivo. *J Clin Endocrinol Metab* 82: 4196–4200, 1997.
37. **Moller DE, Berger JP.** Role of PPARs in the regulation of obesity-related insulin sensitivity and inflammation. *Int J Obes Relat Metab Disord* 27 *Suppl* 3: S17–21, 2003.
38. **Montague CT, O'Rahilly S.** The perils of portliness: causes and consequences of visceral adiposity. *Diabetes* 49: 883–888, 2000.
39. **Morton NM, Paterson JM, Masuzaki H, Holmes MC, Staels B, Fievet C, Walker BR, Flier JS, Mullins JJ, Seckl JR.** Novel adipose tissue-mediated resistance to diet-induced visceral obesity in 11β-hydroxysteroid dehydrogenase type 1-deficient mice. *Diabetes* 53: 931–938, 2004.
40. **Muller S, Martin S, Koenig W, Hanifi-Moghaddam P, Rathmann W, Haastert B, Giani G, Illig T, Thorand B, Kolb H.** Impaired glucose tolerance is associated with increased serum concentrations of interleukin 6 and co-regulated acute-phase proteins but not TNF-alpha or its receptors. *Diabetologia* 45: 805–812, 2002.
41. **Napolitano A, Voice MW, Edwards CR, Seckl JR, Chapman KE.** 11beta-hydroxysteroid dehydrogenase 1 in adipocytes: expression is differentiation-dependent and hormonally regulated. *J Steroid Biochem Mol Biol* 64: 251–260, 1998.
42. **Ohara Y, Peterson TE, Harrison DG.** Hypercholesterolemia increases endothelial superoxide anion production. *J Clin Invest* 91: 2546–2551, 1993.
43. **Pape ME, Kim KH.** Effect of tumor necrosis factor on acetyl-coenzyme A carboxylase gene expression and preadipocyte differentiation. *Mol Endocrinol* 2: 395–403, 1988.
44. **Paulmyer-Lacroix O, Boullu S, Oliver C, Alessi MC, Grino M.** Expression of the mRNA coding for 11beta-hydroxysteroid dehydrogenase type 1 in adipose tissue from obese patients: an in situ hybridization study. *J Clin Endocrinol Metab* 87: 2701–2705, 2002.
45. **Perreault M, Marette A.** Targeted disruption of inducible nitric oxide synthase protects against obesity-linked insulin resistance in muscle. *Nat Med* 7: 1138–1143, 2001.
46. **Petruschke T, Hauner H.** Tumor necrosis factor-alpha prevents the differentiation of human adipocyte precursor cells and causes delipidation of newly developed fat cells. *J Clin Endocrinol Metab* 76: 742–747, 1993.
47. **Pickup JC, Mattock MB, Chusney GD, Burt D.** NIDDM as a disease of the innate immune system: association of acute-phase reactants and interleukin-6 with metabolic syndrome X. *Diabetologia* 40: 1286–1292, 1997.
48. **Poulain-Godefroy O, Froguel P.** Preadipocyte response and impairment of differentiation in an inflammatory environment. *Biochem Biophys Res Commun* 356: 662–667, 2007.
49. **Rhen T, Cidlowski JA.** Antiinflammatory action of glucocorticoids–new mechanisms for old drugs. *N Engl J Med* 353: 1711–1723, 2005.
50. **Roberge C, Carpentier AC, Langlois MF, Baillargeon JP, Ardilouze JL, Maheux P, Gallo-Payet N.** Adrenocortical dysregulation as a major player in insulin resistance and onset of obesity. *Am J Physiol Endocrinol Metab* 293: E1465–E1478, 2007.
51. **Sakaue H, Ogawa W, Matsumoto M, Kuroda S, Takata M, Sugimoto T, Spiegelman BM, Kasuga M.** Posttranscriptional control of adipocyte differentiation through activation of phosphoinositide 3-kinase. *J Biol Chem* 273: 28945–28952, 1998.
52. **Sandeep TC, Andrew R, Homer NZ, Andrews RC, Smith K, Walker BR.** Increased in vivo regeneration of cortisol in adipose tissue in human obesity and effects of the 11beta- hydroxysteroid dehydrogenase type 1 inhibitor carbenoxolone. *Diabetes* 54: 872–879, 2005.
53. **Schaffler A, Scholmerich J, Buchler C.** Mechanisms of disease: adipocytokines and visceral adipose tissue–emerging role in intestinal and mesenteric diseases. *Nat Clin Pract Gastroenterol Hepatol* 2: 103–111, 2005.
54. **Seckl JR, Walker BR.** Minireview: 11beta-hydroxysteroid dehydrogenase type 1- a tissue-specific amplifier of glucocorticoid action. *Endocrinology* 142: 1371–1376, 2001.
55. **Smoak KA, Cidlowski JA.** Mechanisms of glucocorticoid receptor signaling during inflammation. *Mech Ageing Dev* 125: 697–706, 2004.
56. **Straub RH, Hense HW, Andus T, Scholmerich J, Riegger GA, Schunkert H.** Hormone replacement therapy and interrelation between serum interleukin-6 and body mass index in postmenopausal women: a population-based study. *J Clin Endocrinol Metab* 85: 1340–1344, 2000.
57. **Tchkonia T, Giorgadze N, Pirtskhalava T, Thomou T, DePonte M, Koo A, Forse RA, Chinnappan D, Martin-Ruiz C, von Zglinicki T, Kirkland JL.** Fat depot-specific characteristics are retained in strains derived from single human preadipocytes. *Diabetes* 55: 2571–2578, 2006.
58. **Tilg H, Moschen AR.** Adipocytokines: mediators linking adipose tissue, inflammation and immunity. *Nat Rev Immunol* 6: 772–783, 2006.
59. **Tontonoz P, Hu E, Graves RA, Budavari AI, Spiegelman BM.** mPPAR gamma 2: tissue-specific regulator of an adipocyte enhancer. *Genes Dev* 8: 1224–1234, 1994.
60. **Ulick S, Tedde R, Mantero F.** Pathogenesis of the type 2 variant of the syndrome of apparent mineralocorticoid excess. *J Clin Endocrinol Metab* 70: 200–206, 1990.
61. **Wake DJ, Rask E, Livingstone DE, Soderberg S, Olsson T, Walker BR.** Local and systemic impact of transcriptional up-regulation of 11beta-hydroxysteroid dehydrogenase type 1 in adipose tissue in human obesity. *J Clin Endocrinol Metab* 88: 3983–3988, 2003.
62. **Wamil M, Andrew R, Chapman KE, Street J, Morton NM, Seckl JR.** 7-oxysterols modulate glucocorticoid activity in adipocytes through competition for 11beta-hydroxysteroid dehydrogenase type. *Endocrinology* 149: 5909–5918, 2008.
63. **Weisberg SP, McCann D, Desai M, Rosenbaum M, Leibel RL, Ferrante AW Jr.** Obesity is associated with macrophage accumulation in adipose tissue. *J Clin Invest* 112: 1796–1808, 2003.
64. **Xing H, Northrop JP, Grove JR, Kilpatrick KE, Su JL, Ringold GM.** TNF alpha-mediated inhibition and reversal of adipocyte differentiation is accompanied by suppressed expression of PPARg without effects on Pref-1 expression. *Endocrinology* 138: 2776–2783, 1997.
65. **Xu H, Barnes GT, Yang Q, Tan G, Yang D, Chou CJ, Sole J, Nichols A, Ross JS, Tartaglia LA, Chen H.** Chronic inflammation in fat plays a crucial role in the development of obesity-related insulin resistance. *J Clin Invest* 112: 1821–1830, 2003.
66. **Yeager MP, Guyre PM, Munck AU.** Glucocorticoid regulation of the inflammatory response to injury. *Acta Anaesthesiol Scand* 48: 799–813, 2004.
67. **Zhang TY, Daynes RA.** Glucocorticoid conditioning of myeloid progenitors enhances TLR4 signaling via negative regulation of the phosphatidylinositol 3-kinase-Akt pathway. *J Immunol* 178: 2517–2526, 2007.

Am J Physiol Endocrinol Metab 299: E142, 2010;
doi:10.1152/ajpendo.zh1-6016-corr.2010.

Volume 298, May 2010

Ishii-Yonemoto T, Masuzaki H, Yasue S, Okada S, Kozuka C, Tanaka T, Noguchi M, Tomita T, Fujikura J, Yamamoto Y, Ebihara K, Hosoda K, Nakao K. Glucocorticoid reamplification within cells intensifies NF-κB and MAPK signaling and reinforces inflammation in activated preadipocytes. *Am J Physiol Endocrinol Metab* 298: E930-E940, 2010. First published September 23, 2009; doi:10.1152/ajpendo.00320.2009; http://ajpendo.physiology.org/cgi/content/full/298/5/E930.

Originally, blots in Figures 2, 3, 4, 5 and 6 were adjusted to show representative blots without demarcation. Revised Figures 2, 3, 4, 5, and 6 are now presented showing representative blots that are clearly separated. 11β-HSD1 activity analyses were performed by running the samples in triplicate under the same conditions as done previously. Independent experiments were performed to confirm the reproducibility of the results. These new figures appear online, linked directly to the article (http://ajpendo.physiology.org/cgi/content/full/ajpendo.00320.2009/DC2). The authors apologize for the previous errors, none of which have altered the conclusions reached in this study.